MAR 2 3 1961

C. 1

NASA TN D-780

NASA TN D-780

TECHNICAL NOTE

D-780

A METHOD FOR OBTAINING THE NONLINEAR AERODYNAMIC STABILITY CHARACTERISTICS OF BODIES OF REVOLUTION FROM FREE-FLIGHT TESTS

By Donn B. Kirk

Ames Research Center
Moffett Field, Calif.

LIBRARY COPY
MAR 24 1961
SPACE FLIGHT
LANGLEY FIELD, VIRGINIA

NATIONAL AERONAUTICS AND SPACE ADMINISTRATION
WASHINGTON March 1961

1V

NATIONAL AERONAUTICS AND SPACE ADMINISTRATION

TECHNICAL NOTE D-780

A METHOD FOR OBTAINING THE NONLINEAR AERODYNAMIC STABILITY CHARACTERISTICS OF BODIES OF REVOLUTION FROM FREE-FLIGHT TESTS

By Donn B. Kirk

SUMMARY

A method is presented for obtaining the nonlinear aerodynamic stability characteristics of bodies of revolution from free-flight tests. The necessary conditions for the application of this method are (1) that the roll rate and damping encountered in a single cycle of oscillation be small, and (2) that the resulting motion be reasonably planar. Four approximations to the nonlinear restoring moment are considered and solutions are obtained in closed form:

1. A single-term polynomial in an arbitrary power of the angle of attack
2. A two-term polynomial having linear and cubic terms
3. A three-term polynomial having linear, cubic, and quintic terms
4. A three-term polynomial having linear, quadratic, and cubic terms

An iteration procedure is formulated to allow the use of each of these approximations for obtaining the aerodynamic coefficients of bodies of revolution from free-flight test data. It is found that although the equations that are solved pertain strictly to planar motion, the solutions are applicable to motions that deviate to a fairly large degree from planar motion.

Two of the approximations are applied to a set of data gathered from the Ames Supersonic Free-Flight Wind Tunnel. It is shown that one of these approximations is clearly superior to the other in fitting the basic data. The results of this better approximation are then compared with both data obtained from a wind tunnel and the results of two other methods for reducing free-flight data. All of these comparisons indicate that the present method yields realistic results. In addition, the results obtained by the present method are considered to be more valid in most cases than the results obtained by the other methods and at least as valid in all cases.

INTRODUCTION

A test conducted in a free-flight ballistic range ordinarily yields the following basic data:

1. The location of the model center of gravity in space as a function of time at a finite number of points
2. The angles of attack, yaw, and roll as functions of time at a finite number of points

From these basic data, other information such as the velocity as a function of time (or distance) and the period of the resulting oscillation can be determined.

A
4
7
9

The problem of obtaining the aerodynamic coefficients from these data involves writing down the equations of motion and solving this set, if possible, using the given data. In the most general case, no solution to the equations of motion exists. It therefore becomes necessary to make certain assumptions, and hence simplify the equations to a set that can be solved.

One assumption that is commonly made to simplify the equations of motion is that the restoring moment is linear with respect to angle of attack. Under this assumption, a number of solutions to the problem do exist (e.g., ref. 1). It has been found, however, that bodies of revolution at high Mach numbers, especially blunt-nosed slender bodies, experience extremely nonlinear restoring moments. It is thus necessary, in order to treat bodies of this type, to discard the assumption of a linear restoring moment and to investigate under what conditions and with what assumptions a solution to the nonlinear case can be obtained.

A variety of solutions to this problem exist (e.g., refs. 2 and 3). However, for a set of data obtained in the Ames Supersonic Free-Flight Wind Tunnel, the adequacy of these known methods was either doubtful or unknown. It was thus decided to attempt to gain better insight into the problem of analyzing the motion of a body governed by a nonlinear restoring moment. A systematic description of this investigation will be given in this report. Attention is first concentrated on a very simple nonlinear case. After examination of this solution, the development will proceed step by step to more complicated cases, eventually arriving at solutions that can be applied to free-flight data with a great deal of confidence.

SYMBOLS

A constant in equations (8), (17), and (25)

B constant in equation (1)

C_m	restoring moment coefficient, $\frac{M}{qSl}$
C_{m_α}	moment-curve slope, $\frac{dC_m}{d\alpha}$
$C_{m_{\alpha_L}}$	moment-curve slope obtained from linear theory (defined in eq. (6))
$F(\varphi,k)$	incomplete elliptic integral of the first kind
g	quantity introduced in obtaining the solutions to a number of integrals (defined in text for the various cases encountered)
h	constant in equation (25)
I	moment of inertia about an axis through the center of gravity and normal to the axis of symmetry
$K(k)$	complete elliptic integral of the first kind
k	modulus of elliptic integral (defined in text for the various cases encountered)
l	reference length
M	restoring moment
m	constant in equations (8), (17), and (25)
n	constant in equation (17)
p	exponent in equation (1)
q	dynamic pressure, $\frac{1}{2}\rho V^2$
R	$\frac{A}{qSl}$
S	reference area
T	period of oscillation
t	time
u	factor appearing in expressions for α_E (defined in text for the various cases encountered)

V	velocity
x	$\left(\frac{\alpha}{\alpha_m}\right)^2$
x_1, x_2	roots of the polynomial appearing in equation (19)
y	$\frac{\alpha}{\alpha_m}$
y_1, y_2, y_3	roots of the polynomial appearing in equation (26)
α	angle of attack
α_E	effective angle of attack (the true value of C_{m_α} at $\alpha = \alpha_E$ is equal to $C_{m_{\alpha_L}}$ at $\alpha = \alpha_m$)
α_m	maximum angle of attack (Note that when "reasonably planar motion" is considered, α_m refers to the maximum <u>resultant</u> angle of attack.)
α_o	minimum resultant angle of attack
β	angle of sideslip
$\beta(a,b)$	beta function
$\Gamma(a)$	gamma function
φ	argument of elliptic integral (defined in text for the various cases encountered)
$(\dot{\ })$	$\frac{d}{dt}(\ )$
$(\ddot{\ })$	$\frac{d^2}{dt^2}(\ )$

A
4
7
9

SOLUTIONS TO THE PROBLEM

Testing of bodies of revolution in the Ames Supersonic Free-Flight Wind Tunnel has indicated that the following conditions are satisfied in many cases:

1. The roll rate of the model is small.
2. The damping of the resulting motion is extremely small when a single cycle of oscillation is considered.
3. The resulting motion of the model is reasonably planar. (The definition that is herein adopted of "reasonably planar motion" is a motion which has the ratio $\alpha_o/\alpha_m < 0.3$ and which roughly describes an ellipse in the α, β plane.)

It will be assumed in the developments to follow that the roll rate and damping are identically zero and that the motion is identically planar. However, the solutions will be considered applicable if the conditions given above are satisfied.

Moment Consisting of a Single Term in an Arbitrary Power of α

A simple nonlinear case that we can consider is one where the moment[1] can be represented as

$$M = C_m qSl = -B\alpha^p \qquad p \geq 1 \tag{1}$$

hence

$$C_{m_\alpha} = -\frac{Bp\alpha^{p-1}}{qSl} \tag{2}$$

Given planar motion, with zero roll rate and damping, our equation of motion to be solved is

$$I\ddot{\alpha} - M = 0$$

or

$$I\ddot{\alpha} + B\alpha^p = 0$$

---

[1] It should be realized that the desired moment is an odd function $[M(-\alpha) = -M(\alpha)]$ which does not follow from equation (1). The derivation that follows, however, does not depend on this point.

On multiplying this equation by $\dot{\alpha}$ and integrating, we obtain

$$\frac{I\dot{\alpha}^2}{2} + \frac{B\alpha^{p+1}}{p + 1} = C$$

To find C, we use the fact that $\dot{\alpha} = 0$ when $\alpha = \alpha_m$. Thus

$$C = \frac{B\alpha_m^{p+1}}{p + 1}$$

and

$$\dot{\alpha} = \frac{d\alpha}{dt} = \sqrt{\frac{2B}{(p + 1)I}\left(\alpha_m^{p+1} - \alpha^{p+1}\right)}$$

A479

$$dt = \sqrt{\frac{(p + 1)I}{2B}}\,\frac{d\alpha}{\sqrt{\alpha_m^{p+1} - \alpha^{p+1}}} \tag{3}$$

We can determine $T/4$ (where T is the period of the oscillation) by integrating equation (3) from $\alpha = 0$ to $\alpha = \alpha_m$; that is,

$$\int_0^{t_m} dt = \frac{T}{4} = \sqrt{\frac{(p + 1)I}{2B}}\int_0^{\alpha_m} \frac{d\alpha}{\sqrt{\alpha_m^{p+1} - \alpha^{p+1}}}$$

This integration can be performed by employing the beta function

$$\beta(a,b) = \int_0^1 u^{a-1}(1 - u)^{b-1}du \qquad \begin{cases} a > 0 \\ b > 0 \end{cases}$$

Thus by letting

$$u = \left(\frac{\alpha}{\alpha_m}\right)^{p+1}$$

$$du = \frac{(p + 1)\alpha^p}{\alpha_m^{p+1}}\,d\alpha = \frac{(p + 1)u^{\frac{p}{p+1}}d\alpha}{\alpha_m}$$

we get

$$\frac{T}{4} = \sqrt{\frac{(p + 1)I}{2B}}\int_0^1 \frac{\alpha_m du}{(p + 1)u^{\frac{p}{p+1}}\sqrt{\alpha_m^{p+1} - \alpha_m^{p+1}u}}$$

or

$$T = \sqrt{\frac{8I}{(p + 1)B\alpha_m^{p-1}}}\,\beta\left(\frac{1}{p + 1}, \frac{1}{2}\right)$$

We can now introduce the relationship between the beta function and the gamma function that

$$\beta(a,b) = \frac{\Gamma(a)\Gamma(b)}{\Gamma(a + b)}$$

$$T = \sqrt{\frac{8I}{(p + 1)B\alpha_m^{p-1}}}\,\frac{\Gamma\left(\frac{1}{p + 1}\right)\Gamma\left(\frac{1}{2}\right)}{\Gamma\left(\frac{p + 3}{2p + 2}\right)}$$

A
4
7
9

and since

$$\Gamma\left(\frac{1}{2}\right) = \sqrt{\pi}$$

$$\Gamma(a + 1) = a\Gamma(a)$$

our expression for the period reduces to

$$T = \sqrt{\frac{2\pi I(p + 3)^2}{(p + 1)B\alpha_m^{p-1}}}\,\frac{\Gamma\left(\frac{p + 2}{p + 1}\right)}{\Gamma\left(\frac{3p + 5}{2p + 2}\right)}$$

Solving for B, we get

$$B = \frac{2\pi I(p + 3)^2}{(p + 1)\alpha_m^{p-1}T^2}\left[\frac{\Gamma\left(\frac{p + 2}{p + 1}\right)}{\Gamma\left(\frac{3p + 5}{2p + 2}\right)}\right]^2 \tag{4}$$

Putting equation (4) into equation (2) gives our final expression for C_{m_α}

$$C_{m_\alpha} = -\frac{2\pi p(p + 3)^2}{p + 1}\left[\frac{\Gamma\left(\frac{p + 2}{p + 1}\right)}{\Gamma\left(\frac{3p + 5}{2p + 2}\right)}\right]^2\left(\frac{\alpha}{\alpha_m}\right)^{p-1}\frac{I}{T^2 qSl} \tag{5}$$

and a similar expression can be obtained for C_m.

For this simple case, our problem is thus solved. However, for the more complicated cases to follow that involve more than one unknown, we will have to develop an indirect method of finding the unknowns. Since this indirect method also leads to a better intuitive feel for the problem, it will be developed for this case also. We proceed as follows: Assuming $p = 1$ (linear theory) in equation (5), we get

$$C_{m\alpha} \equiv C_{m\alpha_L} = \frac{-4\pi^2 I}{T^2 q S l} \tag{6}$$

This is the familiar expression for $C_{m\alpha}$ under linear theory and our additional assumptions. Now, it can be argued that there exists an angle of attack (called α_E) through which our model has oscillated at which the local value of $C_{m\alpha}$ is the same as $C_{m\alpha_L}$ obtained from linear theory. To obtain this angle of attack, we equate (5) and (6), substituting α_E for α in equation (5). Thus

A
4
7
9

$$\frac{-2\pi p(p+3)^2}{p+1}\left[\frac{\Gamma\left(\frac{p+2}{p+1}\right)}{\Gamma\left(\frac{3p+5}{2p+2}\right)}\right]^2\left(\frac{\alpha_E}{\alpha_m}\right)^{p-1}\frac{I}{T^2 q S l} = \frac{-4\pi^2 I}{T^2 q S l}$$

from which

$$\frac{\alpha_E}{\alpha_m} = \left\{\frac{2\pi(p+1)}{p(p+3)^2}\left[\frac{\Gamma\left(\frac{3p+5}{2p+2}\right)}{\Gamma\left(\frac{p+2}{p+1}\right)}\right]^2\right\}^{\frac{1}{p-1}} \tag{7}$$

Now, equation (7) tells us that if our model was indeed governed by the restoring moment assumed in equation (1) (consider p as a known value), then we can determine the real angle of attack at which the $C_{m\alpha_L}$ obtained from linear theory is equal to the local value of $C_{m\alpha}$. In effect, the parameter α_E/α_m tells us the transformation from a plot of $C_{m\alpha_L}$ vs. α_m to a plot of $C_{m\alpha}$ vs. α.

Figure 1 shows a plot of α_E/α_m vs. p. It is interesting to note that for a cubic moment ($M = -B\alpha^3$), $C_{m\alpha_L}$, obtained using linear theory, should be applied at $0.489\ \alpha_m$. This is considerably lower than the root mean square value of a sine wave ($0.707\ \alpha_m$) which one might have expected to be a fairly close value.

The downfall of the approximation that was made in equation (1) is that for $p > 1$ the moment-curve slope at $\alpha = 0^\circ$ is 0. This is obviously too severe a restriction to place on our solution. However, it is felt that this simple analysis has led to an intuitive feel for the problem at hand. We will now consider a slightly more complicated case.

Moment Consisting of a Linear and a Cubic Term

This problem has been treated by Rasmussen in reference 2. Rasmussen considered the two-degrees-of-freedom case (no restriction to planar motion) and obtained solutions in closed form. As a step in building up the present method of solution, however, it is necessary to treat this case in the same manner as our previous example. Also, certain approximations made by Rasmussen in simplifying his final results for application purposes can, for the case of planar motion, be applied in their exact form. It should be noted that the exact solutions presented in reference 2, when specialized to the case of planar motion, can be transformed through mathematical manipulations into the same solutions at which we will arrive.

A
4
7
9

Consider the case where the restoring moment governing our model can be represented as

$$M = C_m q S l = -A\alpha - mA\alpha^3 \tag{8}$$

hence

$$C_{m\alpha} = -\frac{A}{qSl}\left(1 + 3m\alpha^2\right) \tag{9}$$

This assumption is more realistic than our first example since, in this case, the moment-curve slope at $\alpha = 0^\circ$ is not in general zero. It should be noted that under this assumption $d^2C_m/d\alpha^2 = 0$ at $\alpha = 0^\circ$. The equation of motion that will be solved is again

$$I\ddot{\alpha} - M = 0$$

or

$$I\ddot{\alpha} + A\alpha + mA\alpha^3 = 0$$

Following exactly the procedure set forth in the first example, we obtain

$$T = \sqrt{32I}\int_0^{\alpha_m} \frac{d\alpha}{\sqrt{A\left(2\alpha_m^2 + m\alpha_m^4 - 2\alpha^2 - m\alpha^4\right)}}$$

or on letting $y = \alpha/\alpha_m$

$$\left.\begin{aligned} T &= \sqrt{\frac{32I}{Am\alpha_m^2}}\int_0^1 \frac{dy}{\sqrt{(1-y^2)\left(y^2+\frac{m\alpha_m^2+2}{m\alpha_m^2}\right)}} \qquad Am > 0 \\ T &= \sqrt{\frac{32I}{-Am\alpha_m^2}}\int_0^1 \frac{dy}{\sqrt{(1-y^2)\left(-y^2-\frac{m\alpha_m^2+2}{m\alpha_m^2}\right)}} \qquad Am < 0 \end{aligned}\right\} \quad (10)$$

A479

Now we must consider the three possible cases that exist under equation (8). These are shown in sketch (a).

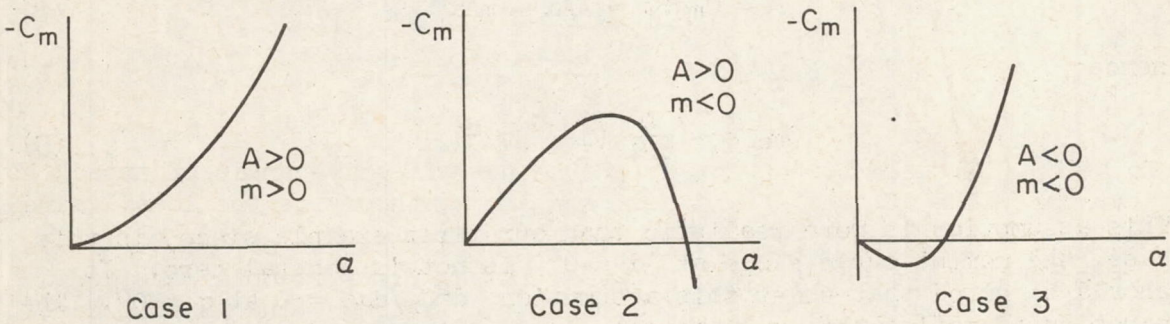

Sketch (a)

Case 1.- Since Am is greater than zero, the first of equations (10) is the appropriate one. With m greater than zero, the polynomial under the radical within the integral in this equation is nowhere negative between the limits of 0 and 1, so we can proceed with the integration. This integration can be performed by using 213.00 from Byrd and Friedman (ref. 4).

$$T = \sqrt{\frac{32I}{Am\alpha_m^2}}\, gK(k)$$

where

$$g^2 = k^2 = \frac{m\alpha_m^2}{2(m\alpha_m^2 + 1)}$$

and $K(k)$ denotes the complete elliptic integral of the first kind. Solving for A, we get

$$A = \frac{32I}{m\alpha_m^2 T^2} g^2[K(k)]^2 \tag{11}$$

Putting equation (11) into equation (9) gives our final expression for C_{m_α}

$$C_{m_\alpha} = \frac{-16[K(k)]^2}{m\alpha_m^2 + 1}(1 + 3m\alpha^2)\frac{I}{T^2 qSl} \tag{12}$$

A
4
7
9

Once again, we solve for the effective angle of attack at which the local value of C_{m_α} is the same as $C_{m_{\alpha_L}}$ obtained from linear theory. Hence, by equating equations (6) and (12), we obtain

$$\alpha_E = \sqrt{\frac{\pi^2(1 + m\alpha_m^2)}{12m[K(k)]^2} - \frac{1}{3m}} \tag{13}$$

Equation (13) tells us how to determine our effective angle of attack so that the value of $C_{m_{\alpha_L}}$ obtained from linear theory is the local value of C_{m_α}. In figure 2, α_E/α_m is plotted as a function of $m\alpha_m^2$. It is noted that the value of 0.489 obtained in the first example considered (where the linear term was neglected) is a limiting value in this case, and nowhere does the shift differ substantially from this value.

Case 2.- In this case, $Am < 0$, so the second of equations (10) is applicable. Before we can proceed with this integration, we must determine under what conditions the polynomial under the radical within the integral is non-negative. If it is negative anywhere between the limits of 0 and 1, the period of the oscillation is imaginary, corresponding to instability. This polynomial can be shown to be non-negative between the given limits, leading to a period that is real and finite, as long as the following condition holds:

$$-1 < m\alpha_m^2 < 0 \tag{14}$$

This can be pictured more clearly be referring to sketch (b). The condition $m\alpha_m^2 = -1$ gives the value of $\alpha_m \equiv \alpha_1$ at which there is an unstable trim point; condition (14) states that $0 < \alpha_m < \alpha_1$. With these thoughts in mind, we can now integrate equation (10) by using 220.00 from reference 4.

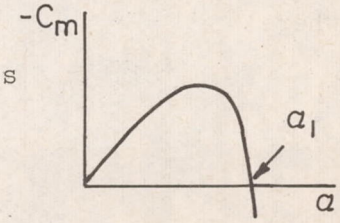

Sketch (b)

$$T = \sqrt{\frac{32I}{-Am\alpha_m^2}}\, gK(k)$$

where

$$g^2 = k^2 = \frac{-m\alpha_m^2}{m\alpha_m^2 + 2}$$

$K(k)$ = complete elliptic integral of the first kind

Solving for A, we get

$$A = \frac{-32I}{m\alpha_m^2 T^2} g^2[K(k)]^2$$

A479

Putting this equation into equation (9) gives the expression for C_{m_α}

$$C_{m_\alpha} = \frac{-32[K(k)]^2}{m\alpha_m^2 + 2}(1 + 3m\alpha^2)\frac{I}{T^2 qSl}$$

The expression for α_E is now obtained by equating this expression with equation (6).

$$\alpha_E = \sqrt{\frac{\pi^2(2 + m\alpha_m^2)}{24m[K(k)]^2} - \frac{1}{3m}} \tag{15}$$

This case is also plotted in figure 2. It is noted that α_E/α_m for this case lies between 0.50 and 0.577.

Case 3.- In this case, $Am > 0$ so equations (10) assume the same form as under Case 1; that is,

$$T = \sqrt{\frac{32I}{Am\alpha_m^2}} \int_0^1 \frac{dy}{\sqrt{(1 - y^2)\left(y^2 + \frac{m\alpha_m^2 + 2}{m\alpha_m^2}\right)}}$$

Here the condition for the quantity under the radical within the integral to be positive or zero between the given limits can be written as

$$\frac{m\alpha_m^2 + 2}{m\alpha_m^2} > 0$$

or

$$m\alpha_m^2 < -2 \tag{16}$$

Physically, what this means can be explained as follows (see sketch (c)). If a model were launched at $\alpha = \alpha_4$, it would continue to fly at that angle of attack throughout its trajectory. Similarly, if launched at α_3, it would oscillate between α_3 and α_5. The area under the curve between α_4 and α_5 is a measure of the energy added to the system while the corresponding area between α_4 and α_3 is a measure of the energy removed from the system. Since we have neglected damping, the model would oscillate between limits that make these areas equal. Now we have insisted that the model oscillate through $\alpha = 0$ (i.e., between $\alpha = \alpha_m$ and $\alpha = -\alpha_m$), which cannot occur unless α_m is large enough to allow the shaded area above $-C_m = 0$ to be equal to that below $-C_m = 0$. Thus, condition (16) does nothing more than state that $\alpha_m > \alpha_2$. With this in mind, we find that the solution to Case 3 is identical to that of Case 1; that is,

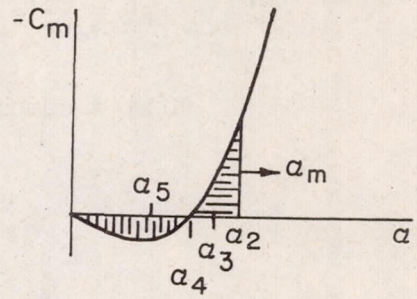

Sketch (c)

A479

$$\alpha_E = \sqrt{\frac{\pi^2(1 + m\alpha_m^2)}{12m[K(k)]^2} - \frac{1}{3m}} \tag{13}$$

where

$$k^2 = \frac{m\alpha_m^2}{2(m\alpha_m^2 + 1)}$$

It is noted from figure 2 that for this case, α_E/α_m varies between 0.408 and 0.489. As in Case 1, throughout most of the range the value obtained when the linear term is neglected (0.489) is a close approximation.

USE OF LINEAR PLUS CUBIC APPROXIMATION

Assume that at least two firings are made of a given configuration in a free-flight facility. Assume also that over one cycle of oscillation the damping is negligible, that the roll rate is small, and that the motion is reasonably planar (see definition, page 5).

It is then an easy matter to determine α_m and to apply linear theory and determine $C_{m\alpha_L}$ for each of the runs. If the data points appear to fall on curves like any of those shown in figure 3, the linear plus cubic approximation can satisfactorily fit the data. It is obvious that if the data show an inflection point or are other than continuously increasing or continuously decreasing, the linear plus cubic approximation cannot fit very well.

Two runs are then chosen which have values of α_m reasonably far apart. We can then obtain two equations with two unknowns by inserting the following into equation (9): Replace

$$C_{m_\alpha} \text{ by } C_{m_{\alpha_L}}$$

$$\alpha \text{ by } \alpha_E$$

and define

$$R = \frac{A}{qSl}$$

Then

A479

$$C_{m_{\alpha_{L_1}}} = -R(1 + 3m\alpha_{E_1}{}^2)$$

$$C_{m_{\alpha_{L_2}}} = -R(1 + 3m\alpha_{E_2}{}^2)$$

In matrix form, these equations become

$$\begin{bmatrix} -C_{m_{\alpha_{L_1}}} \\ -C_{m_{\alpha_{L_2}}} \end{bmatrix} = \begin{bmatrix} 1 & 3\alpha_{E_1}{}^2 \\ 1 & 3\alpha_{E_2}{}^2 \end{bmatrix} \begin{bmatrix} R \\ mR \end{bmatrix}$$

or

$$\begin{bmatrix} -C_{m_{\alpha_L}} \end{bmatrix} = \begin{bmatrix} P \end{bmatrix} \begin{bmatrix} Q \end{bmatrix}$$

Since P is nonsingular, it has a unique inverse, and we can write

$$\begin{bmatrix} P^{-1} \end{bmatrix} \begin{bmatrix} -C_{m_{\alpha_L}} \end{bmatrix} = \begin{bmatrix} P^{-1} \end{bmatrix} \begin{bmatrix} P \end{bmatrix} \begin{bmatrix} Q \end{bmatrix} = \begin{bmatrix} Q \end{bmatrix}$$

We are thus led to the following expression for the unknown coefficients:

$$\begin{bmatrix} R \\ mR \end{bmatrix} = \begin{bmatrix} \dfrac{-\alpha_{E_2}{}^2}{\alpha_{E_1}{}^2 - \alpha_{E_2}{}^2} & \dfrac{\alpha_{E_1}{}^2}{\alpha_{E_1}{}^2 - \alpha_{E_2}{}^2} \\ \dfrac{1}{3(\alpha_{E_1}{}^2 - \alpha_{E_2}{}^2)} & \dfrac{-1}{3(\alpha_{E_1}{}^2 - \alpha_{E_2}{}^2)} \end{bmatrix} \begin{bmatrix} -C_{m_{\alpha_{L_1}}} \\ -C_{m_{\alpha_{L_2}}} \end{bmatrix}$$

It will be obvious from a plot of $C_{m_{\alpha_L}}$ vs. α_m whether the test results qualify for Case 2 or for Cases 1 and 3 (see fig. 3).

After choosing the governing case, it then becomes merely a matter of assuming a value of α_E (anything near $0.5\ \alpha_m$ is sufficiently close), determining the P^{-1} matrix using equation (13) or (15), and from this forming the Q matrix. The quantity m is obviously mR/R.

This new value of m is used to obtain a new P^{-1} matrix and the iteration process continues. The iteration process converges very rapidly for each of the three cases. After m and R are obtained, C_m, as a function of α, is determined from equation (8).

After the iteration process has converged, the solution will of necessity go through the two data points used. The demonstration of the adequacy of the linear plus cubic moment assumption is in how well the curve goes through additional data points obtained from testing the same configuration. This is checked by constructing the $C_{m_{\alpha_L}}$ vs. α_m curve from the following equation, using the values of R and m given by the iteration process:

A
4
7
9

$$C_{m_{\alpha_L}} = -R(1 + 3m\alpha_E^2)$$

If this leads to a reasonable fit of the data points, a better fit can be obtained in the following manner. First a least squares fit is obtained of $C_{m_{\alpha_L}}$ vs. α_m having the same form as equation (9).

$$C_{m_{\alpha_L}} = a + b\alpha_m^2$$

After solving for a and b, two points are chosen from this least squares fit to use as inputs for the iteration procedure. The iteration procedure will then yield a fit of the data points that falls very close to the least squares fit. This could best be termed a quasi least squares procedure.

Moment Consisting of a Linear, a Cubic, and a Quintic Term

Next, consider the case where the restoring moment governing our model can be represented as

$$M = C_m qSl = -A\alpha - mA\alpha^3 - nA\alpha^5 \tag{17}$$

hence

$$C_{m_\alpha} = -\frac{A}{qSl}\left(1 + 3m\alpha^2 + 5n\alpha^4\right) \tag{18}$$

Once again it is noted that $\frac{d^2C_m}{d\alpha^2} = 0$ at $\alpha = 0^\circ$. The equation of motion that will be solved is

$$I\ddot{\alpha} - M = 0$$

or

$$I\ddot{\alpha} + A\alpha + mA\alpha^3 + nA\alpha^5 = 0$$

A
4
7
9

Again we follow exactly the procedure set forth in the first example considered and obtain

$$T = \sqrt{96I}\int_0^{\alpha_m} \frac{d\alpha}{\sqrt{A(6\alpha_m^2 + 3m\alpha_m^4 + 2n\alpha_m^6 - 6\alpha^2 - 3m\alpha^4 - 2n\alpha^6)}}$$

or on letting $x = \left(\frac{\alpha}{\alpha_m}\right)^2$

$$T = \sqrt{\frac{12I}{\alpha_m^4}}\int_0^1 \frac{dx}{\sqrt{An\left\{x(1-x)\left[x^2 + \left(\frac{3m\alpha_m^2 + 2n\alpha_m^4}{2n\alpha_m^4}\right)x + \left(\frac{6 + 3m\alpha_m^2 + 2n\alpha_m^4}{2n\alpha_m^4}\right)\right]\right\}}} \tag{19}$$

We will define by x_1 and x_2 the roots to the quadratic polynomial that appears in the denominator of our integral.

$$x_1 = \frac{-(3m + 2n\alpha_m^2) + \sqrt{9m^2 - 48n - 12mn\alpha_m^2 - 12n^2\alpha_m^4}}{4n\alpha_m^2}$$

$$x_2 = \frac{-(3m + 2n\alpha_m^2) - \sqrt{9m^2 - 48n - 12mn\alpha_m^2 - 12n^2\alpha_m^4}}{4n\alpha_m^2}$$

These roots may be both real or both complex. Now, equation (19) may be rewritten in the following manner.

$$\left.\begin{aligned} T &= \sqrt{\frac{12I}{An\alpha_m^4}}\int_0^1 \frac{dx}{\sqrt{x(1-x)(x-x_1)(x-x_2)}} \qquad An > 0 \\ T &= \sqrt{\frac{12I}{-An\alpha_m^4}}\int_0^1 \frac{dx}{\sqrt{-x(1-x)(x-x_1)(x-x_2)}} \qquad An < 0 \end{aligned}\right\} \quad (20)$$

The quantity under the radical outside the integral is then always positive. To obtain a meaningful solution to equations (20), it is necessary for the quantity under the other radical to be non-negative between the given limits. This condition will be discussed when the individual cases that exist under equation (17) are considered. These cases are shown in figure 4.

Case 1: Linear, cubic, and quintic terms are all stabilizing ($A > 0$, $m > 0$, $n > 0$).- The first thing we must determine is under what conditions the polynomial under the radical within the integral in the first of equations (20) is non-negative between the limits 0 and 1.

Assume first that x_1 and x_2 are real (i.e., $9m^2 - 48n - 12mn\alpha_m^2 - 12n^2\alpha_m^4 > 0$). This can obviously be achieved by making m large and n small. Under this assumption, it is apparent that $x_1 > x_2$ and that $x_2 < 0$. To show that $x_1 < 0$, rewrite the expression for x_1 as follows:

$$x_1 = \frac{-\sqrt{9m^2+12mn\alpha_m^2+4n^2\alpha_m^4} + \sqrt{(9m^2+12mn\alpha_m^2+4n^2\alpha_m^4) - (48n+24mn\alpha_m^2+16n^2\alpha_m^4)}}{4n\alpha_m^2}$$

Since the expression under the first radical is larger than that under the second radical and the denominator is positive, $x_1 < 0$. Now, since $x_2 < x_1 < 0$, the terms $(x - x_1)$ and $(x - x_2)$ are necessarily positive between the given limits and the expression under the radical is > 0 between these limits. We thus have the following (see sketch (d)):

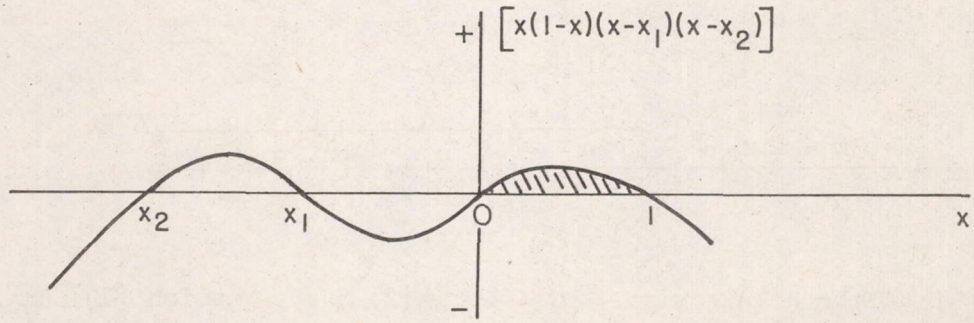

Sketch (d)

Next, assume that x_1 and x_2 are complex (i.e., $9m^2 - 48n - 12mn\alpha_m^2 - 12n^2\alpha_m^4 < 0$). This can obviously be achieved by making n large and m small.

Now, x_1 and x_2 can be expressed as follows:

$$x_1 = \frac{-a + i\sqrt{b}}{c}$$

$$x_2 = \frac{-a - i\sqrt{b}}{c}$$

with $a > 0$, $b > 0$, $c > 0$. Then the product $(x - x_1)(x - x_2)$ has the following expansion:

$$(x - x_1)(x - x_2) = x^2 + \frac{2ax}{c} + \frac{a^2}{c^2} + \frac{b}{c^2}$$

This term is positive for $0 \leq x \leq 1$, and hence the term in the denominator of our integral is ≥ 0 between the given limits. We thus have the following (see sketch (e)):

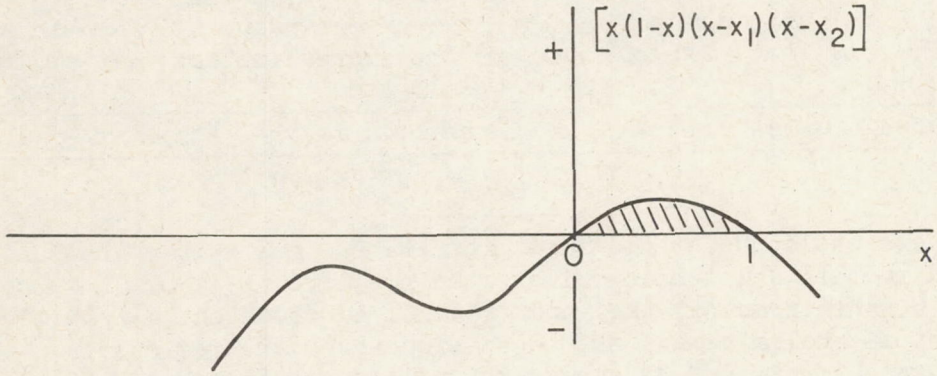

Sketch (e)

We can now proceed to solve equations (20). The two subcases of Case 1 will be treated separately.

Subcase 1, x_1 and x_2 real: Making use of 256.00 from reference 4, we can write

$$T = \sqrt{\frac{12I}{An\alpha_m^4}}\, gK(k)$$

where

$$g^2 = \frac{4}{x_1x_2 - x_2}$$

$$k^2 = \frac{x_1 - x_2}{x_1x_2 - x_2}$$

Solving for A, we get

$$A = \frac{12I}{n\alpha_m{}^4T^2}\, g^2[K(k)]^2$$

Putting this equation into equation (18) gives the expression for $C_{m\alpha}$

$$C_{m\alpha} = -\frac{12g^2[K(k)]^2}{n\alpha_m{}^4}\,(1 + 3m\alpha^2 + 5n\alpha^4)\,\frac{I}{T^2qSl}$$

The expression for α_E is now obtained by equating this expression with equation (6).

$$\alpha_E = \sqrt{\frac{-3m + \sqrt{9m^2 - 20n(1 - u)}}{10n}} \tag{21}$$

where

$$u = \frac{\pi^2 n\alpha_m{}^4}{3g^2[K(k)]^2}$$

The plus sign in front of the inner radical in equation (21) is chosen in order for α_E to be real.

Subcase 2, x_1 and x_2 complex: Applying 259.00 from reference 4, we can write

$$T = \sqrt{\frac{48I}{An\alpha_m{}^4}}\, gK(k)$$

where

$$g^2 = \frac{1}{\sqrt{x_1x_2(1 - x_1 - x_2 + x_1x_2)}}$$

$$= \frac{n\alpha_m{}^4}{\sqrt{\frac{3}{2}\,(1 + m\alpha_m{}^2 + n\alpha_m{}^4)(6 + 3m\alpha_m{}^2 + 2n\alpha_m{}^4)}}$$

$$k^2 = \frac{1}{2} + \frac{x_1 + x_2 - 2x_1x_2}{4\sqrt{x_1x_2(1 - x_1 - x_2 + x_1x_2)}}$$

$$= \frac{1}{2} - \frac{3}{4}\frac{(4 + 3m\alpha_m^2 + 2n\alpha_m^4)}{\sqrt{6(1 + m\alpha_m^2 + n\alpha_m^4)(6 + 3m\alpha_m^2 + 2n\alpha_m^4)}}$$

Solving for A, we get

$$A = \frac{48I}{n\alpha_m^4T^2} g^2[K(k)]^2$$

Putting this expression into equation (18) gives the expression for C_{m_α}.

$$C_{m_\alpha} = \frac{-48g^2[K(k)]^2}{n\alpha_m^4}(1 + 3m\alpha^2 + 5n\alpha^4)\frac{I}{T^2qSl}$$

Equating this expression with equation (6) gives the expression for α_E.

$$\alpha_E = \sqrt{\frac{-3m + \sqrt{9m^2 - 20n(1 - u)}}{10n}} \tag{22}$$

where

$$u = \frac{\pi^2 n\alpha_m^4}{12g^2[K(k)]^2}$$

It is noted that equation (22) has the same form as equation (21), but it should be kept in mind that u, g, and k are expressed differently in the two subcases.

General discussion concerning additional cases.- A rigorous derivation of the expression for α_E for each of the additional cases that exist under equation (17) would consume much space and serve little purpose. The form of this expression for each case can be written as

$$\alpha_E = \sqrt{\frac{-3m \pm \sqrt{9m^2 - 20n(1 - u)}}{10n}} \tag{23}$$

The appropriate expressions for u, g, and k vary depending on whether x_1 and x_2 are real or complex and also on the case under consideration. We will define a number of u, g, and k which will allow us to indicate in tabular form the appropriate expressions to use.

$$u_1 = \frac{\pi^2 n\alpha_m^4}{3g^2[K(k)]^2} \qquad u_2 = \frac{-\pi^2 n\alpha_m^4}{3g^2[K(k)]^2} \qquad u_3 = \frac{\pi^2 n\alpha_m^4}{12g^2[K(k)]^2}$$

$$g_1^2 = \frac{4}{|x_1x_2 - x_2|} \qquad g_2^2 = \frac{4}{|x_1x_2 - x_1|}$$

$$g_3^2 = \frac{n\alpha_m^4}{\sqrt{\frac{3}{2}(1 + m\alpha_m^2 + n\alpha_m^4)(6 + 3m\alpha_m^2 + 2n\alpha_m^4)}}$$

A479

$$k_1 = \left|\frac{x_2 - x_1}{x_1x_2 - x_2}\right| \qquad k_2 = \left|\frac{x_2 - x_1}{x_1x_2 - x_1}\right|$$

$$k_3 = \sqrt{\frac{1}{2} - \frac{3(4 + 3m\alpha_m^2 + 2n\alpha_m^4)}{4\sqrt{6(1 + m\alpha_m^2 + n\alpha_m^4)(6 + 3m\alpha_m^2 + 2n\alpha_m^4)}}}$$

TABLE I

Case	Description	x_1 and x_2	u	g^2	k	Valid root (eq. (23))	α_1, α_2
1	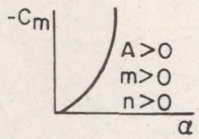	Real or Complex	u_1 / u_3	g_1^2 / g_3^2	k_1 / k_3	+	
2.1	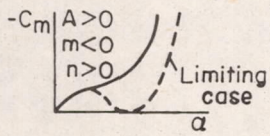	Complex only	u_3	g_3^2	k_3	+ Always - Sometimes	
2.2	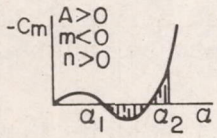	Real or Complex	u_1 / u_3	g_1^2 / g_3^2	k_1 / k_3	+ Always - Sometimes	$\alpha_1 = \sqrt{\frac{-m - \sqrt{m^2-4n}}{2n}}$ $\alpha_2 = \sqrt{\frac{-m + 2\sqrt{m^2-4n}}{2n}}$
3	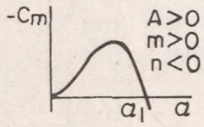	Real only	u_2	g_1^2	k_1	- Always + Sometimes	$\alpha_1 = \sqrt{\frac{-m - \sqrt{m^2-4n}}{2n}}$

TABLE I - Concluded

Case	Description	x_1 and x_2	u	g^2	k	Valid root (eq. (23))	α_1, α_2
4	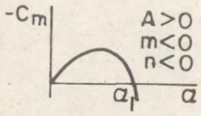	Real only	u_2	g_1^2	k_1	-	$\alpha_1 = \sqrt{\frac{-m - \sqrt{m^2-4n}}{2n}}$
5	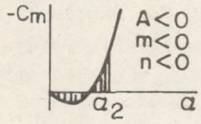	Real or Complex	u_1 u_3	g_2^2 g_3^2	k_2 k_3	-	$\alpha_2 = \sqrt{\frac{-3m - \sqrt{9m^2-48n}}{4n}}$
6	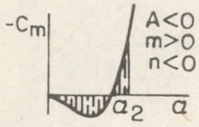	Real or Complex	u_1 u_3	g_2^2 g_3^2	k_2 k_3	-	$\alpha_2 = \sqrt{\frac{-3m - \sqrt{9m^2-48n}}{4n}}$
7	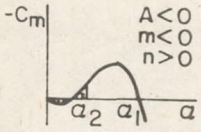	Real only	u_2	g_2^2	k_2	Both always	$\alpha_1 = \sqrt{\frac{-m + \sqrt{m^2-4n}}{2n}}$ $\alpha_2 = \sqrt{\frac{-3m - \sqrt{9m^2-48n}}{4n}}$

A479

The column headed "valid root" denotes the appropriate sign to be used in front of the inner radical in equation (23). Some cases can have two valid roots because of the double-valued nature of C_{m_α}. It is clear from sketch (f) that there are two transformations that can be applied to point A that will place it on the C_{m_α} vs. α curve, while only one such transformation exists for point C. The point labeled B is evidently the dividing point between these two possibilities.

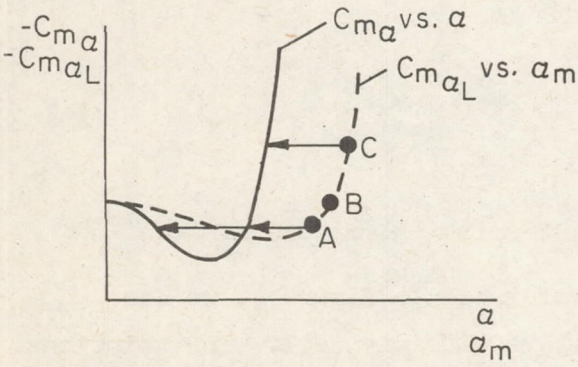

Sketch (f)

The tabulated values of α_1 and α_2 indicate the dividing line between regions where our solution does and does not exist. Specifically, we must insist that $\alpha_m < \alpha_1$ and/or $\alpha_m > \alpha_2$. If these conditions are not satisfied, the quantity under the radical within the integral in equations (20) becomes negative and the solution that has been developed has no meaning. The physical meaning of these conditions can be realized by noting that

we have insisted that the model oscillate through $\alpha = 0^{\circ}$ and, if the conditions are not satisfied, this will not be the case. It should be noted that α_1 is an unstable trim point and that α_2 is located so that the shaded areas above and below $-C_m = 0$ are equal.

USE OF THE LINEAR PLUS CUBIC PLUS QUINTIC APPROXIMATION

Before this approximation can be applied, at least three firings of a given configuration must have been made. We then proceed as in the case of the linear plus cubic approximation (page 13) and obtain three equations with three unknowns. These equations can be written in matrix form as follows:

$$\begin{bmatrix} -C_{m_{\alpha_{L_1}}} \\ -C_{m_{\alpha_{L_2}}} \\ -C_{m_{\alpha_{L_3}}} \end{bmatrix} = \begin{bmatrix} 1 & 3\alpha_{E_1}^{\ 2} & 5\alpha_{E_1}^{\ 4} \\ 1 & 3\alpha_{E_2}^{\ 2} & 5\alpha_{E_2}^{\ 4} \\ 1 & 3\alpha_{E_3}^{\ 2} & 5\alpha_{E_3}^{\ 4} \end{bmatrix} \begin{bmatrix} R \\ mR \\ nR \end{bmatrix}$$

Once again we determine the inverse of the square matrix, and we can then write

$$\begin{bmatrix} R \\ mR \\ nR \end{bmatrix} = \begin{bmatrix} \dfrac{\alpha_{E_2}^{\ 2}\alpha_{E_3}^{\ 2}}{(\alpha_{E_1}^{\ 2} - \alpha_{E_2}^{\ 2})(\alpha_{E_1}^{\ 2} - \alpha_{E_3}^{\ 2})} & \dfrac{-\alpha_{E_1}^{\ 2}\alpha_{E_3}^{\ 2}}{(\alpha_{E_1}^{\ 2} - \alpha_{E_2}^{\ 2})(\alpha_{E_2}^{\ 2} - \alpha_{E_3}^{\ 2})} & \dfrac{\alpha_{E_1}^{\ 2}\alpha_{E_2}^{\ 2}}{(\alpha_{E_1}^{\ 2} - \alpha_{E_3}^{\ 2})(\alpha_{E_2}^{\ 2} - \alpha_{E_3}^{\ 2})} \\ -\dfrac{1}{3}\dfrac{\alpha_{E_2}^{\ 2} + \alpha_{E_3}^{\ 2}}{(\alpha_{E_1}^{\ 2} - \alpha_{E_2}^{\ 2})(\alpha_{E_1}^{\ 2} - \alpha_{E_3}^{\ 2})} & \dfrac{1}{3}\dfrac{\alpha_{E_1}^{\ 2} + \alpha_{E_3}^{\ 2}}{(\alpha_{E_1}^{\ 2} - \alpha_{E_2}^{\ 2})(\alpha_{E_2}^{\ 2} - \alpha_{E_3}^{\ 2})} & -\dfrac{1}{3}\dfrac{\alpha_{E_1}^{\ 2} + \alpha_{E_2}^{\ 2}}{(\alpha_{E_1}^{\ 2} - \alpha_{E_3}^{\ 2})(\alpha_{E_2}^{\ 2} - \alpha_{E_3}^{\ 2})} \\ \dfrac{1}{5(\alpha_{E_1}^{\ 2} - \alpha_{E_2}^{\ 2})(\alpha_{E_1}^{\ 2} - \alpha_{E_3}^{\ 2})} & \dfrac{-1}{5(\alpha_{E_1}^{\ 2} - \alpha_{E_2}^{\ 2})(\alpha_{E_2}^{\ 2} - \alpha_{E_3}^{\ 2})} & \dfrac{1}{5(\alpha_{E_1}^{\ 2} - \alpha_{E_3}^{\ 2})(\alpha_{E_2}^{\ 2} - \alpha_{E_3}^{\ 2})} \end{bmatrix} \begin{bmatrix} -C_{m_{\alpha_{L_1}}} \\ -C_{m_{\alpha_{L_2}}} \\ -C_{m_{\alpha_{L_3}}} \end{bmatrix} \tag{24}$$

From equations (24), we would like to determine R, m, and n.

From a plot of $C_{m_{\alpha_L}}$ vs. α_m and reference to figure 4, we can determine the cases under which our test results may fall. The solutions are so similar that it need not concern us that we are unable to pinpoint a specific case that governs our data. This is especially true if the problem is programmed for a digital computer. It is fairly easy to set up a general program that will handle all possible cases.

A guess is now made at values of m, n, and R (only a positive or negative sign need be assigned to R) and an iteration process is started. From m, n, and R, the three values of α_E can be determined from equation (23) and the information in table I. When more than one root of equation (23) is valid, the root that gives the largest spread between the highest and lowest values of α_E should be used. Sketch (g) clarifies this. It is apparent that the points A, B, and C better define the C_{m_α} vs. α curve than do the points A, B, and D. Equations (24) can then be solved for R, mR, and nR, and hence for m and n. These new values of m, n, and R are used to obtain new values of the α_E, and the iteration process continues.

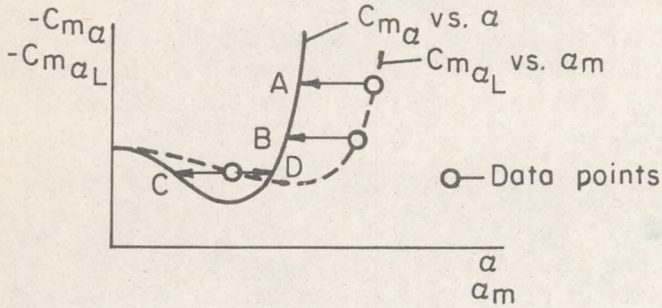

Sketch (g)

A479

It has been found that the iteration process converges very rapidly for all cases that are initially stable (Cases 1 through 4), even with extremely poor initial guesses of m and n. The same is unfortunately not true for cases that are initially unstable (Cases 5 through 7). For these cases the iteration process diverges, even with almost exact guesses of m and n. This condition can be remedied to some extent as follows: We will make the assumption that R (i.e., $-C_{m_\alpha}$ at $\alpha = 0^\circ$) is a known value and will then proceed to obtain expressions for m and n. Only two data points will be used to get these values; the third data point will be used in a way that is explained presently.

Regarding R as known, our two equations are

$$\begin{bmatrix} -\left(\dfrac{C_{m_{\alpha_{L_1}}}}{R} + 1\right) \\ -\left(\dfrac{C_{m_{\alpha_{L_2}}}}{R} + 1\right) \end{bmatrix} = \begin{bmatrix} 3\alpha_{E_1}^2 & 5\alpha_{E_1}^4 \\ 3\alpha_{E_2}^2 & 5\alpha_{E_2}^4 \end{bmatrix} \begin{bmatrix} m \\ n \end{bmatrix}$$

By determining the inverse of the square matrix that appears above, we can write

$$\begin{bmatrix} m \\ n \end{bmatrix} = \begin{bmatrix} \dfrac{\alpha_{E_2}^2}{3\alpha_{E_1}^2(\alpha_{E_1}^2 - \alpha_{E_2}^2)} & \dfrac{-\alpha_{E_1}^2}{3\alpha_{E_2}^2(\alpha_{E_1}^2 - \alpha_{E_2}^2)} \\ \dfrac{-1}{5\alpha_{E_1}^2(\alpha_{E_1}^2 - \alpha_{E_2}^2)} & \dfrac{1}{5\alpha_{E_2}^2(\alpha_{E_1}^2 - \alpha_{E_2}^2)} \end{bmatrix} \begin{bmatrix} \dfrac{C_{m_{\alpha_{L_1}}}}{R} + 1 \\ \dfrac{C_{m_{\alpha_{L_2}}}}{R} + 1 \end{bmatrix}$$

Now we can make a guess of m and n and go through an iteration process as before. In this case the convergence is rapid if the assumed value of R is anywhere reasonably close to its true value.

This process is repeated for several different assumed values of R. In each case, after the iteration has converged, we form the following parameter: $\Delta C_{m_{\alpha_L}} = C_{m_{\alpha_L}}$ (known for third data point) - $C_{m_{\alpha_L}}$ (given by iterated solution). Then we can graphically determine a value of R so that the iterated solution will go through all three data points, and with this value of R as an input, the iteration will yield the corresponding values of m and n (see sketch (h)).

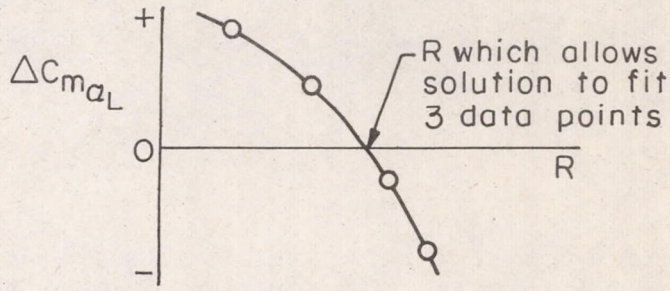

Sketch (h)

A479

Regardless of which case is under consideration, once the iteration process has converged, the solution will of necessity pass through the three given data points. The adequacy of the 1-3-5 approximation is determined by seeing how well it fits additional data points obtained from tests of the same configuration. The $C_{m_{\alpha_L}}$ vs. α_m curve is constructed from the following equation using the values of R, m, and n given by the iteration process:

$$C_{m_{\alpha_L}} = -R(1 + 3m\alpha_E^2 + 5n\alpha_E^4)$$

Once again, a better fit can be obtained by using the quasi least squares procedure mentioned on page 15. For this approximation, a least squares fit of the form

$$C_{m_{\alpha_L}} = a + b\alpha_m^2 + c\alpha_m^4$$

is obtained, and then three points from this fit are used as inputs for the iteration procedure.

Moment Consisting of a Linear, a Quadratic, and a Cubic Term

Next consider the case where the restoring moment[2] governing our model can be represented as

$$M = C_m q S l = -A\alpha - hA\alpha^2 - mA\alpha^3 \tag{25}$$

hence

$$C_{m_\alpha} = \frac{-A}{qSl}\left(1 + 2h\alpha + 3m\alpha^2\right)$$

For a moment of this type, it is noted that $d^2C_m/d\alpha^2$ is not, in general, zero at $\alpha = 0^\circ$. The equation of motion that will be solved is A479

$$I\ddot{\alpha} - M = 0$$

or

$$I\ddot{\alpha} + A\alpha + hA\alpha^2 + mA\alpha^3 = 0$$

Again the procedure set forth in the first example that was considered is followed, and we obtain

$$T = \sqrt{96I}\int_0^{\alpha_m} \frac{d\alpha}{\sqrt{A(6\alpha_m^2 + 4h\alpha_m^3 + 3m\alpha_m^4 - 6\alpha^2 - 4h\alpha^3 - 3m\alpha^4)}}$$

or on letting $y = \alpha/\alpha_m$

$$\left.\begin{aligned}
T &= \sqrt{\frac{32I}{Am\alpha_m^2}}\int_0^1 \frac{dy}{\sqrt{(1-y)\left[y^3 + \left(\frac{3m\alpha_m^2 + 4h\alpha_m}{3m\alpha_m^2}\right)y^2 + \left(\frac{3m\alpha_m^2 + 4h\alpha_m + 6}{3m\alpha_m^2}\right)y + \left(\frac{3m\alpha_m^2 + 4h\alpha_m + 6}{3m\alpha_m^2}\right)\right]}} \qquad Am > 0 \\
T &= \sqrt{\frac{32I}{-Am\alpha_m^2}}\int_0^1 \frac{dy}{\sqrt{(y-1)\left[y^3 + \left(\frac{3m\alpha_m^2 + 4h\alpha_m}{3m\alpha_m^2}\right)y^2 + \left(\frac{3m\alpha_m^2 + 4h\alpha_m + 6}{3m\alpha_m^2}\right)y + \left(\frac{3m\alpha_m^2 + 4h\alpha_m + 6}{3m\alpha_m^2}\right)\right]}} \qquad Am < 0
\end{aligned}\right\} \tag{26}$$

---

[2]It should be realized that the desired moment is an odd function and that to be strictly correct we should write $\alpha|\alpha|$ for the quadratic term. This does not make any difference in our derivation and hence will not be carried through.

We will define by y_1, y_2, and y_3 the roots of the cubic polynomial that appear in the denominator of our integral. Since these roots may all be real or one may be real and two complex, they will be defined as follows:

> If there is only one real root, this root is defined as y_1. No distinction between y_2 and y_3 is necessary. If there are three real roots, they are defined such that $y_1 > y_2 > y_3$.

To obtain expressions for the three roots, it is convenient to define the following quantities:

A
4
7
9

$$c = \frac{4h}{3m\alpha_m} + 1$$

$$d = \frac{6}{3m\alpha_m^2}$$

$$G_o = \frac{1}{54}\left(2c^3 - 9c^2 + 27c - 9cd + 27d\right)$$

$$H_o = \frac{1}{9}\left(3c + 3d - c^2\right)$$

$$G = \sqrt[3]{-G_o + \sqrt{G_o^2 + H_o^3}}$$

$$H = \sqrt[3]{-G_o - \sqrt{G_o^2 + H_o^3}}$$

$$\mu = \cos^{-1}\left(\mp\sqrt{\frac{-G_o^2}{H_o^3}}\right) \qquad \begin{array}{l} - \text{ if } G_o > 0 \\ + \text{ if } G_o < 0 \\ 0^\circ < \mu < 180^\circ \end{array}$$

Then, if $G_o^2 + H_o^3 > 0$, there are one real root and two complex roots

$$\left.\begin{aligned} y_1 &= G + H - \frac{c}{3} \\ y_{2,3} &= \frac{1}{2}\left[-\left(G + H + \frac{2c}{3}\right) \pm i\sqrt{3}(G - H)\right] \end{aligned}\right\} \qquad (27)$$

If $G_o^2 + H_o^3 < 0$, there are three real roots

$$y_i = -\frac{c}{3} + 2\sqrt{-H_o}\cos\left(\frac{\mu}{3} + 120^\circ p\right) \qquad \left.\begin{array}{l} i = 1 \text{ when } p = 0 \\ i = 2 \text{ when } p = 2 \\ i = 3 \text{ when } p = 1 \end{array}\right\} \qquad (28)$$

Now by making use of 253.00, 255.00, 257.00, 259.00, and 260.00 from reference 4, we can obtain solutions to equations (26). The possible cases that exist under the 1-2-3 approximation are the same as under the 1-3-5 approximation (fig. 4), with the exception that $d^2C_m/d\alpha^2$ is not generally zero at $\alpha = 0^\circ$. The solution for the effective angle of attack for each of the cases of interest can be written in the following form:

$$\alpha_E = \frac{-h \pm \sqrt{h^2 - 3m(1 - u)}}{3m} \tag{29}$$

With the aid of the following definitions, the appropriate expressions for u, g, k, and φ to be used for a particular case can be presented in tabular form.

A
4
7
9

Define

$$g_1^2 = \frac{1}{\sqrt{(1-y_2-y_3+y_2y_3)(y_1^2-y_1y_2-y_1y_3+y_2y_3)}} \qquad y_{1,2,3} \text{ from equations (27)}$$

$$\left.\begin{aligned} g_2^2 &= \frac{4}{(y_1 - 1)(y_2 - y_3)} \\ g_3^2 &= \frac{4}{(y_3 - 1)(y_2 - y_1)} \\ g_4^2 &= \frac{4}{(y_2 - 1)(y_3 - y_1)} \end{aligned}\right\} \qquad y_{1,2,3} \text{ from equation (28)}$$

$$\left.\begin{aligned} k_1^2 &= \frac{1}{2} - \frac{2y_1-y_2-y_3-y_1y_2-y_1y_3+2y_2y_3}{4\sqrt{(1-y_2-y_3+y_2y_3)(y_1^2-y_1y_2-y_1y_3+y_2y_3)}} \\ k_2^2 &= \frac{1}{2} + \frac{2y_1-y_2-y_3-y_1y_2-y_1y_3+2y_2y_3}{4\sqrt{(1-y_2-y_3+y_2y_3)(y_1^2-y_1y_2-y_1y_3+y_2y_3)}} \end{aligned}\right\} \qquad y_{1,2,3} \text{ from equations (27)}$$

$$\left.\begin{aligned} k_3^2 &= \frac{(y_3 - 1)(y_2 - y_1)}{(y_1 - 1)(y_2 - y_3)} \\ k_4^2 &= \frac{(y_2 - 1)(y_3 - y_1)}{(y_3 - 1)(y_2 - y_1)} \\ k_5^2 &= \frac{(y_1 - 1)(y_3 - y_2)}{(y_2 - 1)(y_3 - y_1)} \end{aligned}\right\} \qquad y_{1,2,3} \text{ from equation (28)}$$

$$\left.\begin{aligned}
\varphi_1 &= \cos^{-1}\left(\frac{\sqrt{y_1^2-y_1y_2-y_1y_3+y_2y_3} + y_1\sqrt{1-y_2-y_3+y_2y_3}}{\sqrt{y_1^2-y_1y_2-y_1y_3+y_2y_3} - y_1\sqrt{1-y_2-y_3+y_2y_3}}\right)\\
\varphi_2 &= \cos^{-1}\left(\frac{-\sqrt{y_1^2-y_1y_2-y_1y_3+y_2y_3} + y_1\sqrt{1-y_2-y_3+y_2y_3}}{\sqrt{y_1^2-y_1y_2-y_1y_3+y_2y_3} + y_1\sqrt{1-y_2-y_3+y_2y_3}}\right)
\end{aligned}\right\} \quad y_{1,2,3} \text{ from equations (27)}$$

A479

$$\left.\begin{aligned}
\varphi_3 &= \sin^{-1}\sqrt{\frac{y_3 - y_2}{y_2(y_3 - 1)}}\\
\varphi_4 &= \sin^{-1}\sqrt{\frac{y_2 - y_1}{y_1(y_2 - 1)}}\\
\varphi_5 &= \sin^{-1}\sqrt{\frac{y_1 - y_3}{y_3(y_1 - 1)}}
\end{aligned}\right\} \quad y_{1,2,3} \text{ from equation (28)}$$

$$u_1 = \frac{\pi^2 m\alpha_m^2}{8g^2[2K(k) - F(\varphi,k)]^2}$$

$$u_2 = \frac{-\pi^2 m\alpha_m^2}{8g^2[F(\varphi,k)]^2}$$

$$u_3 = \frac{\pi^2 m\alpha_m^2}{8g^2[F(\varphi,k)]^2}$$

TABLE II

Case	Description	y_1,y_2,y_3 (1)	u	g^2	k	φ	Valid root (eq. (29))	α_1,α_2
1	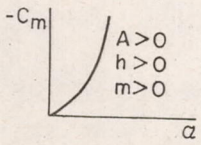	$y_1 < 0$ y_2,y_3 complex	u_1	g_1^2	k_1	φ_1	+	
		or						
		$y_3 < y_2 < y_1 < 0$	u_3	g_4^2	k_5	φ_5		
2.1	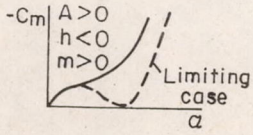	$y_1 < 0$ y_2,y_3 complex	u_1	g_1^2	k_1	φ_1	+ Always - Sometimes	

TABLE II - Concluded

Case	Description	y_1, y_2, y_3 (1)	u	g^2	k	φ	Valid root (eq. (29))	α_1, α_2
2.2	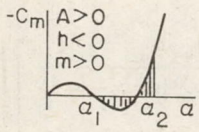	$y_1 < 0$ y_2, y_3 complex or $y_1 > y_2 > 1$ $y_3 < 0$	u_1 u_3	g_1^2 g_2^2	k_1 k_3	φ_1 φ_3	+ Always - Sometimes	$\alpha_1 = \frac{-h-\sqrt{h^2-4m}}{2m}$ (2)
3	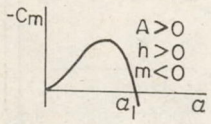	$y_1 > 1$ y_2, y_3 complex or $y_1 > 1$ $y_3 < y_2 < 0$	u_2 u_2	g_1^2 g_3^2	k_2 k_4	φ_2 φ_4	- Always + Sometimes	$\alpha_1 = \frac{-h-\sqrt{h^2-4m}}{2m}$
4	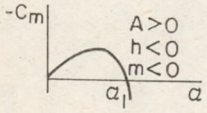	$y_1 > 1$ $y_3 < y_2 < 0$	u_2	g_3^2	k_4	φ_4	-	$\alpha_1 = \frac{-h-\sqrt{h^2-4m}}{2m}$
5	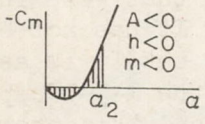	$y_1 < 0$ y_2, y_3 complex	u_1	g_1^2	k_1	φ_1	-	$\alpha_2 = \frac{-2h-\sqrt{4h^2-18m}}{3m}$
6	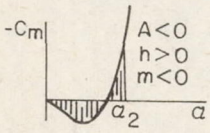	$y_1 < 0$ y_2, y_3 complex	u_1	g_1^2	k_1	φ_1	-	$\alpha_2 = \frac{-2h-\sqrt{4h^2-18m}}{3m}$
7	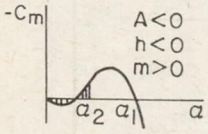	$y_1 > 1$ y_2, y_3 complex	u_2	g_1^2	k_2	φ_2	Both always	$\alpha_1 = \frac{-h+\sqrt{h^2-4m}}{2m}$ $\alpha_2 = \frac{-2h-\sqrt{4h^2-18m}}{3m}$

(1) Everything indicated in this column is correct, but the indicated location of the roots is not necessarily complete. However, all possibilities concerning the roots are covered (except $y_1 > y_2 > y_3 > 1$ which cannot occur) so an additional possibility under any given case can be analyzed by referring to one of the other cases.

(2) $\alpha_2 = \frac{-h + 3\sqrt{h^2 - 4m} + 2\sqrt{h^2 - 3h\sqrt{h^2 - 4m}}}{6m}$

This table has been set up in the same manner as table I (the 1-3-5 polynomial approximation) and a discussion of the significance of the various columns will be found immediately following that table.

A
4
7
9

USE OF THE LINEAR PLUS QUADRATIC PLUS CUBIC APPROXIMATION

The use of this approximation is very similar to use of the 1-3-5 approximation previously discussed, and thus only the pertinent equations will be presented.

$$\begin{bmatrix} R \\ hR \\ mR \end{bmatrix} = \begin{bmatrix} \dfrac{\alpha_{E_2}\alpha_{E_3}}{(\alpha_{E_1} - \alpha_{E_2})(\alpha_{E_1} - \alpha_{E_3})} & \dfrac{-\alpha_{E_1}\alpha_{E_3}}{(\alpha_{E_1} - \alpha_{E_2})(\alpha_{E_2} - \alpha_{E_3})} & \dfrac{\alpha_{E_1}\alpha_{E_2}}{(\alpha_{E_1} - \alpha_{E_3})(\alpha_{E_2} - \alpha_{E_3})} \\ \dfrac{-(\alpha_{E_2} + \alpha_{E_3})}{2(\alpha_{E_1} - \alpha_{E_2})(\alpha_{E_1} - \alpha_{E_3})} & \dfrac{\alpha_{E_1} + \alpha_{E_3}}{2(\alpha_{E_1} - \alpha_{E_2})(\alpha_{E_2} - \alpha_{E_3})} & \dfrac{-(\alpha_{E_1} + \alpha_{E_2})}{2(\alpha_{E_1} - \alpha_{E_3})(\alpha_{E_2} - \alpha_{E_3})} \\ \dfrac{1}{3(\alpha_{E_1} - \alpha_{E_2})(\alpha_{E_1} - \alpha_{E_3})} & \dfrac{-1}{3(\alpha_{E_1} - \alpha_{E_2})(\alpha_{E_2} - \alpha_{E_3})} & \dfrac{1}{3(\alpha_{E_1} - \alpha_{E_3})(\alpha_{E_2} - \alpha_{E_3})} \end{bmatrix} \begin{bmatrix} -C_{m_{\alpha_{L_1}}} \\ -C_{m_{\alpha_{L_2}}} \\ -C_{m_{\alpha_{L_3}}} \end{bmatrix}$$

A479

where α_E is obtained from equation (29).

Once again an iteration process is used to obtain values of R, h, and m. This program has been tried for configurations that were initially stable (Cases 1-4) and was found to converge rapidly. It has not been tried for configurations that were initially unstable, but it is assumed that the iteration process will diverge as it did for the 1-3-5 approximation. If this is the case, the following equations and the scheme indicated in sketch (h) should lead to convergence.

$$\begin{bmatrix} h \\ m \end{bmatrix} = \begin{bmatrix} \dfrac{\alpha_{E_2}}{2\alpha_{E_1}(\alpha_{E_1} - \alpha_{E_2})} & \dfrac{-\alpha_{E_1}}{2\alpha_{E_2}(\alpha_{E_1} - \alpha_{E_2})} \\ \dfrac{-1}{3\alpha_{E_1}(\alpha_{E_1} - \alpha_{E_2})} & \dfrac{1}{3\alpha_{E_2}(\alpha_{E_1} - \alpha_{E_2})} \end{bmatrix} \begin{bmatrix} \dfrac{C_{m_{\alpha_{L_1}}}}{R} + 1 \\ \dfrac{C_{m_{\alpha_{L_2}}}}{R} + 1 \end{bmatrix}$$

RESULTS AND DISCUSSION

Tests conducted in the Ames Supersonic Free-Flight Wind Tunnel of a variety of different models have yielded the following interesting information concerning linear theory. It has been experimentally determined that the application of linear theory to a given model at a given maximum resultant angle of attack will, even for models governed by nonlinear

moments, yield a value of $C_{m_{\alpha_L}}$ that, with certain qualifications, does not depend on the type of motion encountered. These qualifications are that the ratio of α_o/α_m should be less than 0.3 (there is no sudden transition when $\alpha_o/\alpha_m = 0.3$, but above this value the preceding statement becomes questionable), and the resulting motion in the α, β plane should roughly describe an ellipse. When these two conditions are satisfied, the motion is (arbitrarily) defined as reasonably planar motion, and the solutions developed in this report (given in addition small roll rate and damping) will apply. An example of reasonably planar motion is shown in sketch (i) and examples of nonplanar motion are shown in sketches (j) and (k).

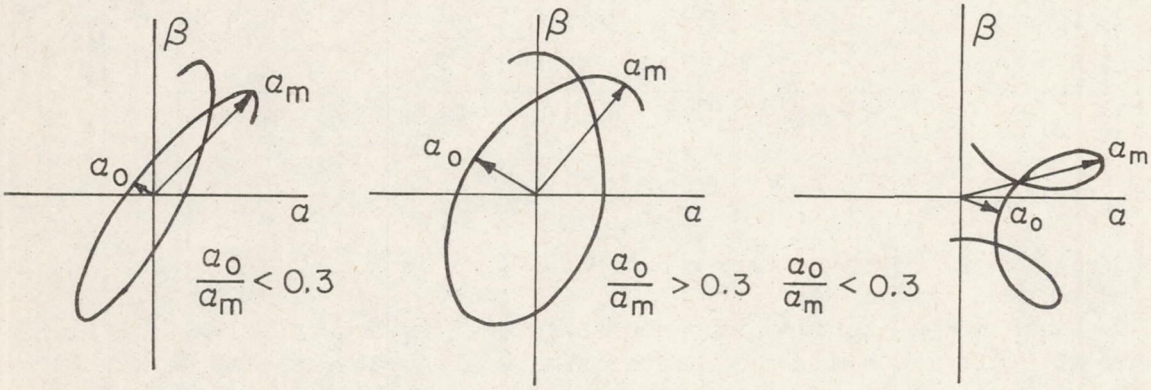

Sketch (i) Sketch (j) Sketch (k)

A 479

A number of shots of a particular blunt-nosed body of revolution were made in the Ames Supersonic Free-Flight Wind Tunnel. The data points obtained from these shots by applying linear theory are shown in figure 5. The ordinate is the moment-curve slope from linear theory and the abscissa is the maximum resultant angle of attack. Each data point represents one shot of the given configuration and all data points were obtained at a Mach number of approximately 11. For each of these shots the ratio of α_o/α_m was less than 0.2, and for the majority of the shots this ratio was less than 0.1. It was hence assumed that the condition of reasonably planar motion was satisfied. Since the roll rate was small and the damping practically zero over one cycle of oscillation, it was concluded that all of the foregoing conditions were satisfied, and the results of the derivations presented in this report could be applied to this collection of data.

The first thing noted from figure 5 is that the moment-curve slope obtained from linear theory appears to get smaller with increasing maximum resultant angle of attack up to about 9° and then increases drastically. This type of behavior eliminates the 1-3 approximation from consideration, since the 1-3 approximation is limited to either a continuously increasing or a continuously decreasing moment-curve slope. However, it is apparent from figure 4 that our data appear to fall under Case 2.1 and that both the 1-3-5 approximation and the 1-2-3 approximation have a chance of adequately fitting the data.

The iteration type of solution that has been described was used to obtain both a 1-3-5 approximation and a 1-2-3 approximation to the given data. These approximations are shown in figure 6. The quasi least squares procedure mentioned on page 25 was used to obtain the fits. It is clear from figure 6 that the 1-3-5 approximation fits the data very well. It is also evident that it is much superior to the 1-2-3 approximation in fitting the data (the two fits had least square values of 0.000985 and 0.00509, respectively). It is felt that this latter conclusion will apply to the majority of configurations encountered since the behavior of most configurations at low angles of attack is fairly linear.

Figure 7 presents curves of the moment coefficient plotted against the true angle of attack corresponding to the two approximations shown in figure 6. Although it has been concluded from figure 6 that the 1-3-5 approximation is superior to the 1-2-3 approximation, it is interesting to note that the two curves in figure 7 show the same general trends and throughout most of the angle-of-attack range agree fairly closely with each other.

A
4
7
9

In figure 8, a comparison is made between free-flight data reduced by using the 1-3-5 approximation and data obtained from tests conducted in the AEDC B-Minor Wind Tunnel. Curves are shown of the moment coefficient plotted against angle of attack at Mach numbers of 5 and 11 from free-flight tests of a given configuration. A corresponding curve at Mach number 8 obtained from wind-tunnel tests is also shown. If it is assumed that the variation of the moment coefficient with Mach number at a given angle of attack is fairly linear, then the wind-tunnel data would be expected to fall about halfway between the two curves of free-flight data. This is essentially borne out throughout most of the angle-of-attack range. It should be noted that the configuration tested in the wind tunnel was very similar, but not identical, to the configuration tested in the free-flight facility. A small difference in the nose shape between these two configurations would be expected to modify the moment coefficient. It is thus felt that the method of reducing the free-flight data by the 1-3-5 approximation has led to a realistic moment curve.

In figure 9, the moment coefficient as a function of angle of attack is shown as obtained from a given set of free-flight data by using the 1-3-5 approximation and by using the method of Rasmussen (ref. 2). The curve showing the 1-3-5 approximation is reproduced from figure 7. The other curve was obtained as follows: A plot was made of $C_{m_{\alpha_L}}$ vs. $(\alpha_m^2 + \alpha_o^2)$. For the method of reference 2 to be directly applicable, this plot should result in a straight line. This was not realized for the given set of data, but is was possible to draw three straight lines that came close to passing through all of the data points (the three lines were determined by least squares fits). The method of reference 2 was then applied individually to each of the three line segments, and the three corresponding segments shown in figure 9 were obtained. It is noted in figure 9 that the two methods yield values of the moment coefficient that remain fairly close to each other throughout the angle-of-attack

range. It is felt, however, that the 1-3-5 approximation is the more applicable of the two methods to the particular set of data considered because of the nonlinearity of the $C_{m_{\alpha_L}}$ vs. $(\alpha_m^2 + \alpha_o^2)$ plot and the accompanying segmented approximation.

Results obtained by using the 1-3-5 approximation are next compared with the corresponding results obtained by using the method of Murphy (ref. 3). To apply this method, the restoring moment is assumed to be linear and the motion in the α, β plane for each run is approximated by an epicycle with damping (two rotating vectors, the tail of one resting on the head of the other). An arbitrary nonlinear moment approximation in odd powers of the resultant angle of attack can then be assumed (i.e., $M = k_1\alpha + k_2\alpha^3 + \ldots$) and solutions for the k_i are obtained from knowledge of the frequencies and lengths of the rotating vectors found in the linearized solution. For a given run, the frequencies are constants and the lengths are approximated by their values at the midpoint of the trajectory.

Several points about this method should be discussed before proceeding:

1. The solutions obtained by Murphy are not exact from a mathematical viewpoint, except for the case of a linear restoring moment. The assumption that an epicycle is the solution to the equation of motion, when the restoring moment is nonlinear, leads to terms which contain mixed frequencies, and these terms are neglected. The resulting solutions can best be described as being the first step in an iteration process.

2. When the 1-3 solution obtained by Murphy is applied to the corresponding case of <u>planar</u> motion, excellent agreement with the exact solution is obtained in most cases. In fact, Murphy's solution corresponds to the line $\alpha_E/\alpha_m = 0.5$ in figure 2, which would lead to reasonable results except in the regions $-1 < m\alpha_m^2 < -0.8$ and $-5 < m\alpha_m^2 < -2$. In these regions the error builds up very rapidly, reaching 100 percent in predicting the period of the resulting oscillation (finite versus infinite) at the points $m\alpha_m^2 = -1, -2$.

3. When the 1-3-5 solution obtained by Murphy is applied to the corresponding case of <u>planar</u> motion, good agreement with the exact solution is obtained in many cases. Because of the number of variables involved, however, it would be very difficult to specify the range of applicability of this approximation as was possible for the 1-3 case. Comparisons have indicated that for this case it is not uncommon for Murphy's method to differ from the exact solution by 10 percent in predicting the period of the oscillation.

In figure 10, the moment coefficient as a function of angle of attack is shown as obtained from the given set of free-flight data by using the 1-3-5 approximation of the present report and by using the method of Murphy

A
4
7
9

(ref. 3). The 1-3 approximation of reference 3 has been used and applied in segments, each segment being determined by a least squares fit. Once again fairly good agreement is obtained throughout the angle-of-attack range.

The same comparison is made in figure 11 as in figure 10 except that the 1-3-5 approximation of reference 3 and an accompanying least squares fit have been used. Although relatively more scatter was found in the experimental data when reduced by the method of reference 3, fairly good agreement between the two methods is noted in this figure. Percentagewise, this comparison indicates about 10 percent difference in the moment coefficient at the highest angle of attack. This is about the same percentage, and in the same direction, that Murphy's solution for the period of the oscillation differs from the exact solution for the corresponding case of planar motion governed by a 1-3-5 moment.

It is perhaps desirable at this time to summarize briefly the advantages and disadvantages of the three methods that have been considered.

1. Rasmussen's method (ref. 2) has the advantages of not being restricted to planar (or reasonably planar) motion and of being an exact solution. It has the disadvantages of being restricted to the 1-3 case only and of being relatively difficult to apply except in its inexact form.

2. Murphy's method (ref. 3) has the advantages of not being restricted to planar (or reasonably planar) motion, of having the widest range of permissible nonlinear moment approximations, and of being relatively easy to apply. It has the disadvantage of being an approximate method from a mathematical viewpoint, with its range of applicability not clearly defined.

3. The method of the present report has the advantages of being an exact solution, of having a fairly wide range of permissible nonlinear moment approximations, and of being relatively easy to apply. It has the disadvantage of being restricted to reasonably planar motion.

CONCLUSIONS

A method has been presented for obtaining the aerodynamic stability characteristics of bodies of revolution that are governed by nonlinear restoring moments from data obtained from free-flight tests. Four different approximations have been presented and solved in closed form. The pertinent conclusions that result from this analysis are as follows:

1. Although the derivations are based on the existence of planar motion, with zero roll rate and damping, the solutions have been found to be applicable when the roll rate and damping are small and when the motion in the α, β plane can be classed as reasonably planar. Under these conditions, the method yields realistic values of the moment coefficient as a function of angle of attack.

2. The various approximations can be programmed for rapid solution on a digital computer with only a modest amount of input information necessary.

3. The resulting solutions are, to a certain extend, self-checking, since only two (or three) data points are used to obtain a given approximation and additional data points can be used to verify the adequacy of the approximation.

A
4
7
9

Ames Research Center
National Aeronautics and Space Administration
Moffett Field, Calif., Jan. 12, 1961

REFERENCES

1. Short, Barbara J., and Sommer, Simon C.: Some Measurements of the Dynamic and Static Stability of Two Blunt-Nosed, Low-Fineness-Ratio Bodies of Revolution in Free Flight at $M = 4$. NASA TM X-20, 1959.

2. Rasmussen, Maurice L.: Determination of Nonlinear Pitching-Moment Characteristics of Axially Symmetric Models From Free-Flight Data. NASA TN D-144, 1960.

3. Murphy, Charles H.: The Measurement of Nonlinear Forces and Moments by Means of Free Flight Tests. BRL Rep. 974, Aberdeen Proving Ground, Feb. 1956.

4. Byrd, Paul F., and Friedman, Morris D.: Handbook of Elliptic Integrals for Engineers and Physicists. Springer-Verlag, Berlin, 1954.

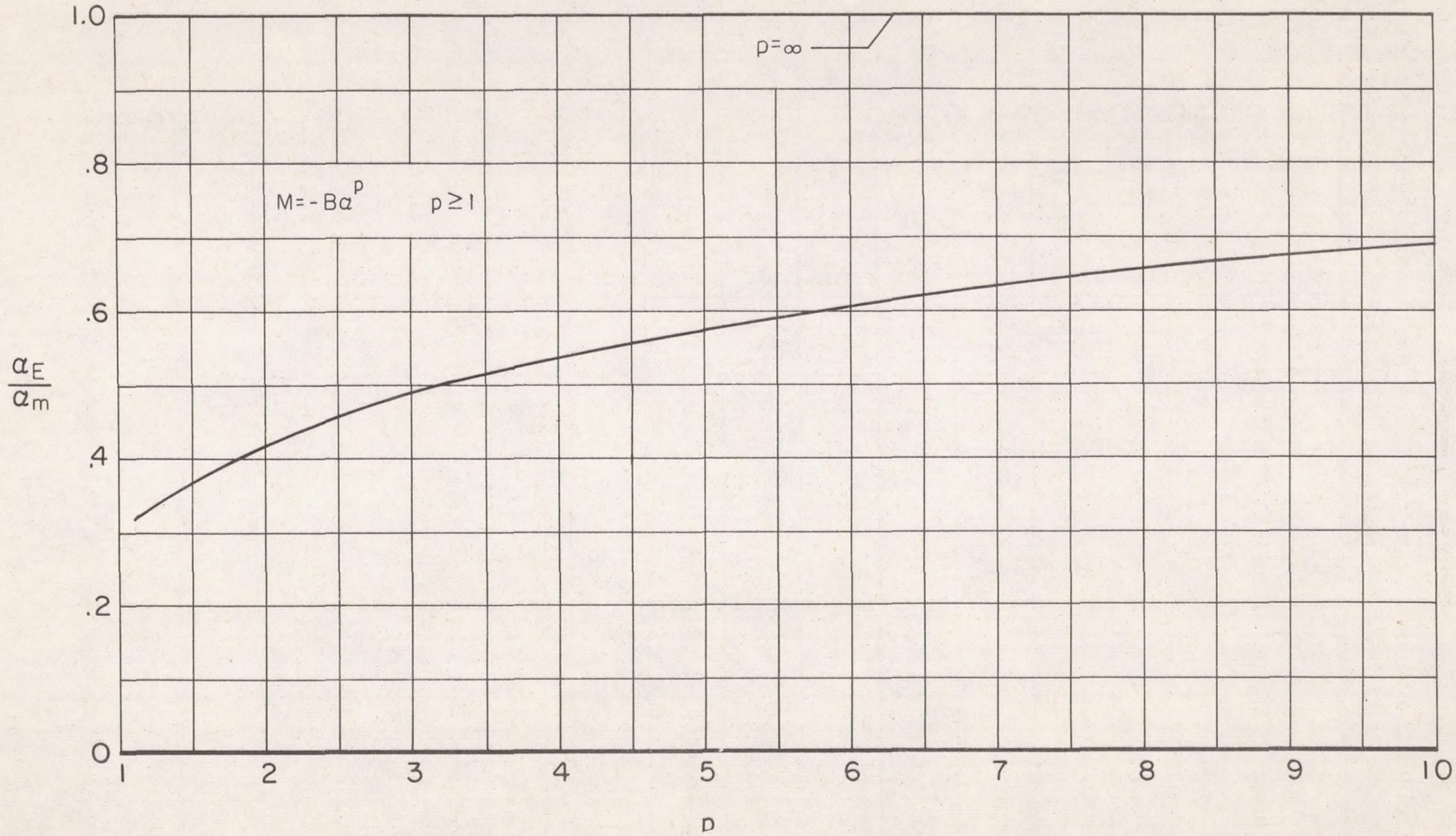

Figure 1.- Effective angle-of-attack parameter for a single term nonlinear restoring moment.

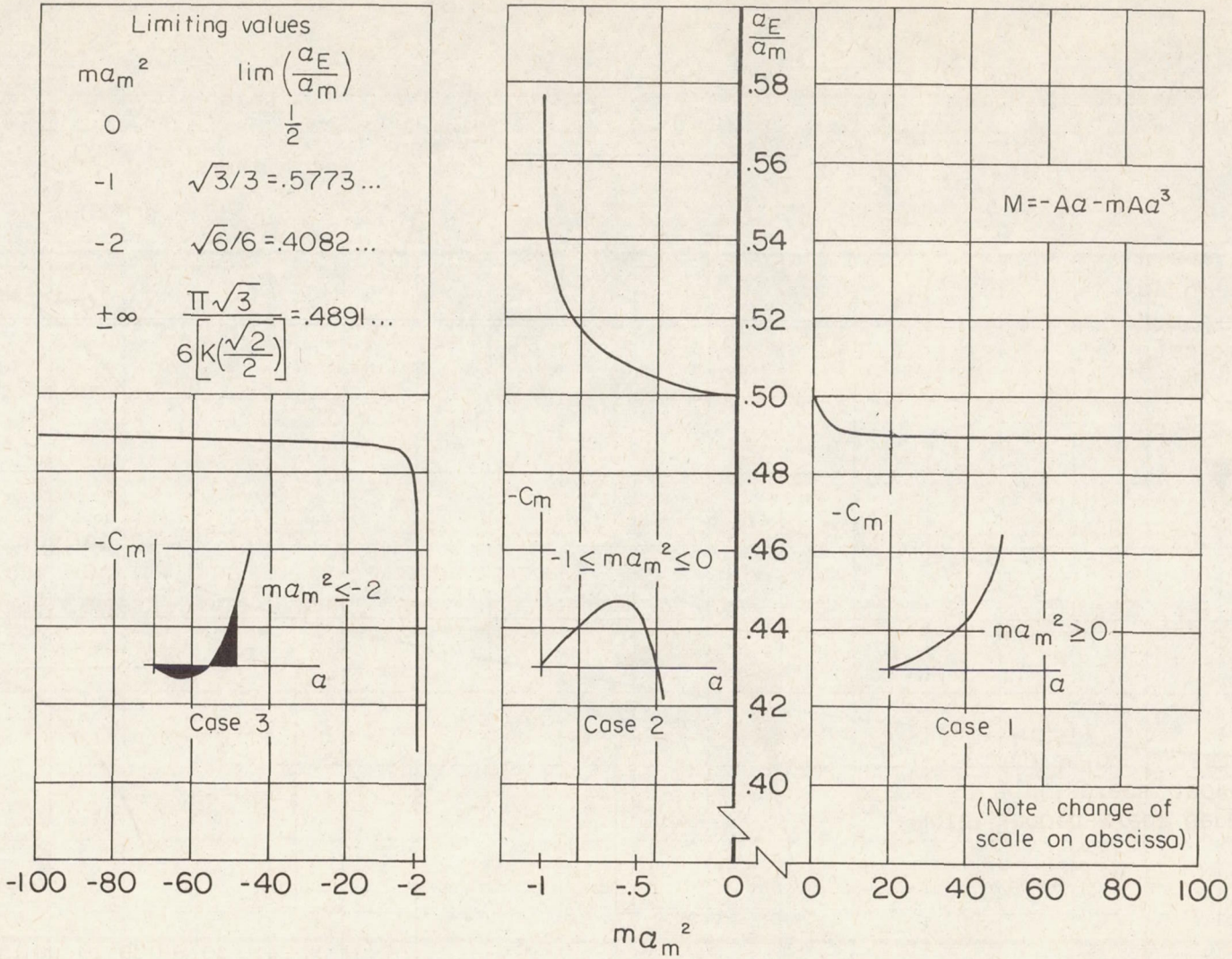

Figure 2.- Effective angle-of-attack parameter for a linear plus cubic restoring moment.

If the moment governing the test configuration as a function of angle of attack is

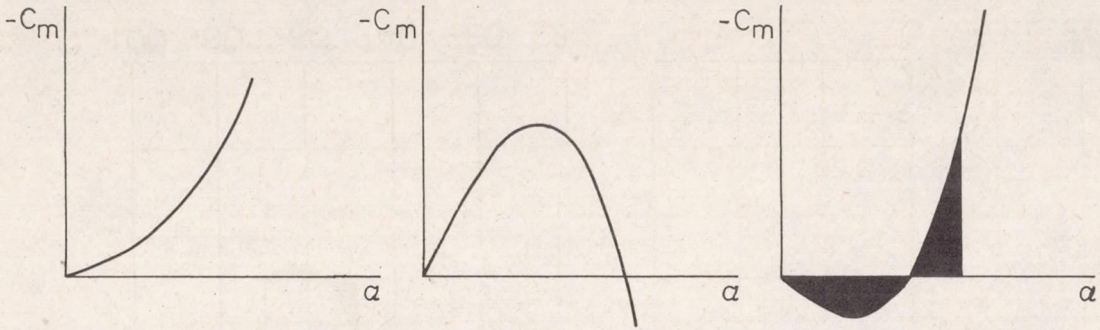

Note: Shaded areas denote equal areas above and below $C_m = 0$

then the corresponding moment curve slope as a function of angle of attack and the moment curve slope obtained from linear theory as a function of α_m are

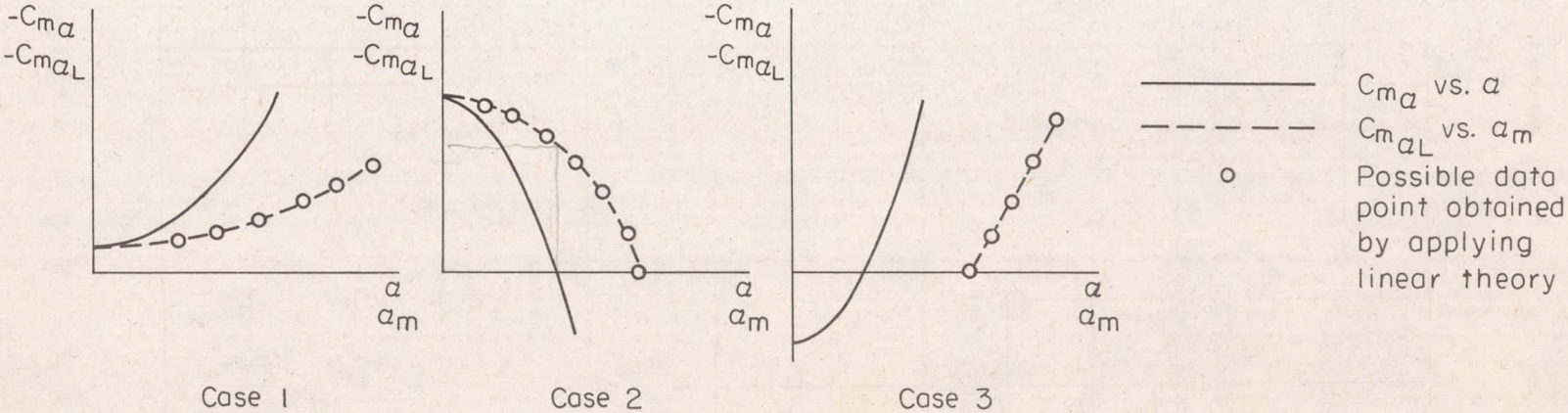

Figure 3.- Cases existing under a linear plus cubic restoring moment assumption.

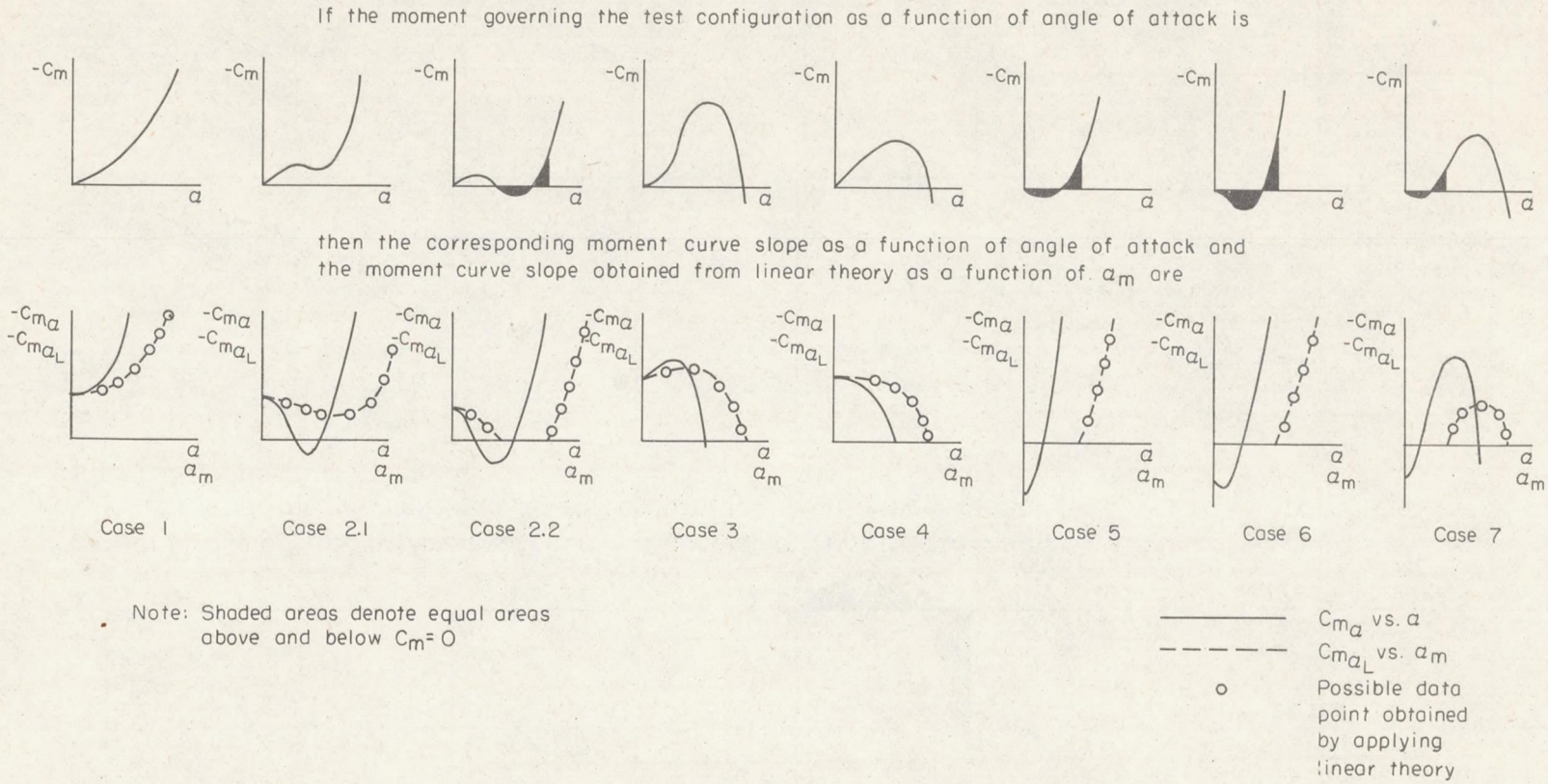

Figure 4.- Cases existing under a 1-3-5 and a 1-2-3 restoring moment assumption.

A
4
7
9

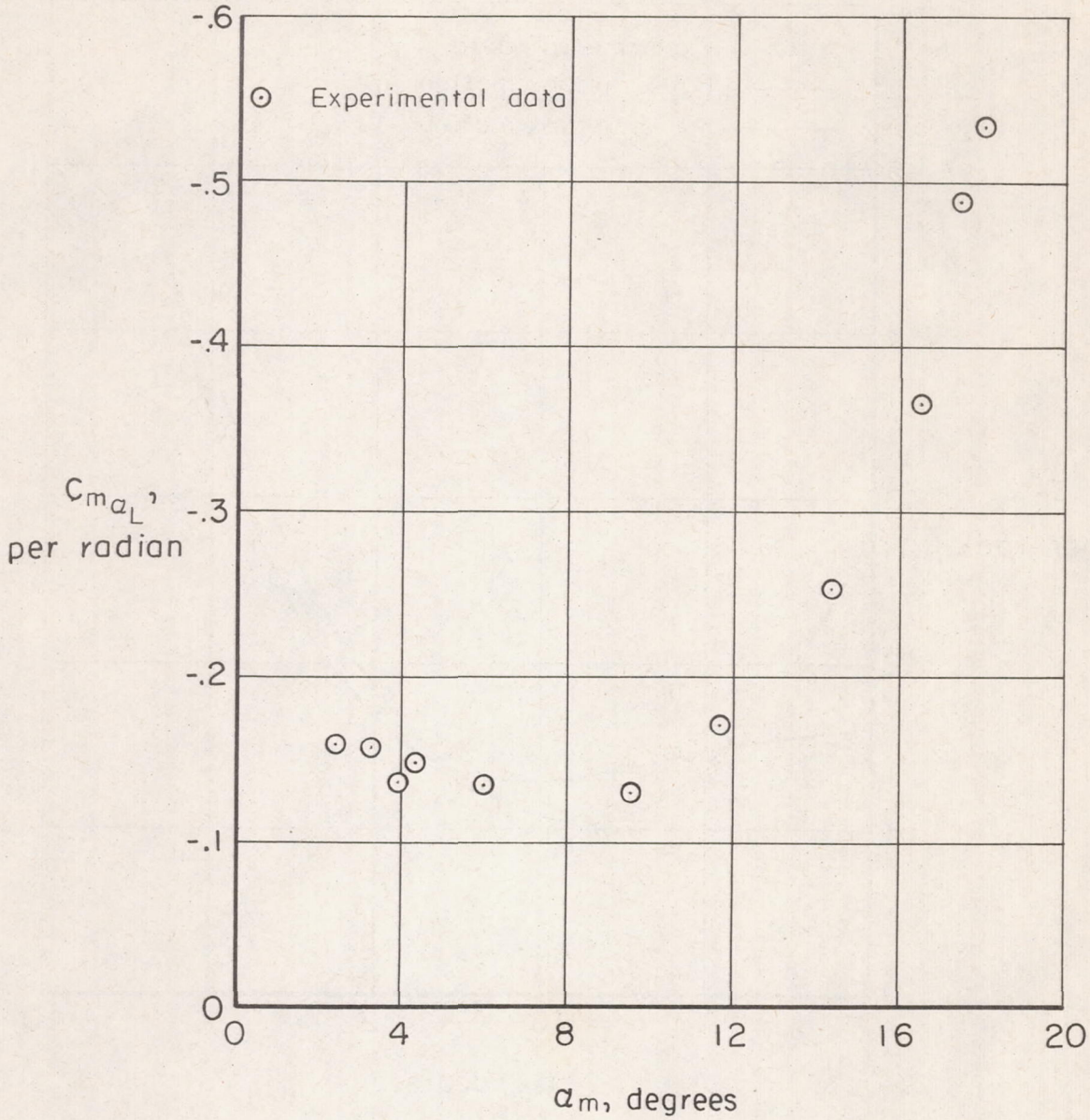

Figure 5.- Moment-curve slope from linear theory as a function of the maximum resultant angle of attack.

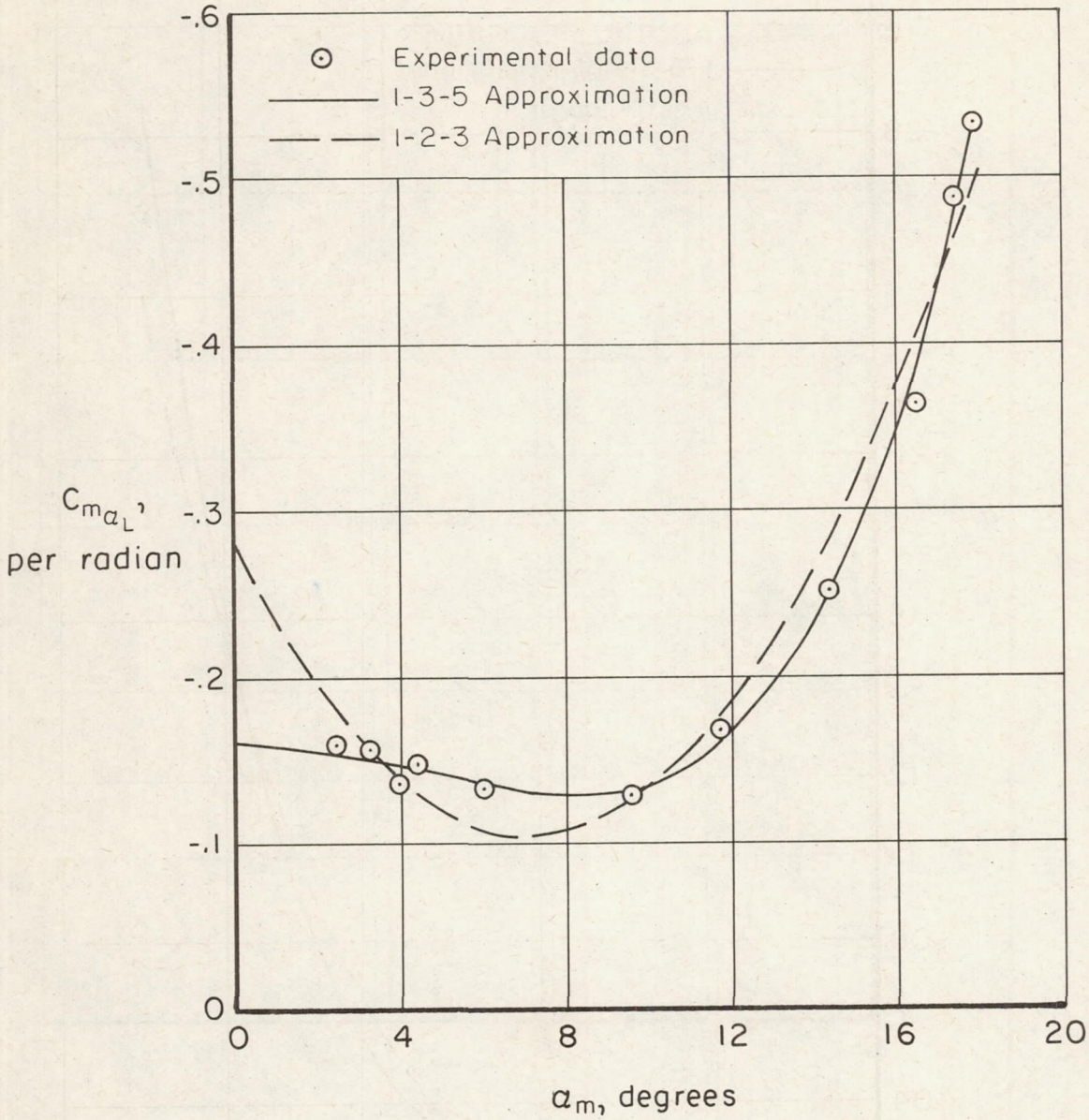

Figure 6.- Comparison of 1-3-5 and 1-2-3 fits of experimental data points.

A
4
7
9

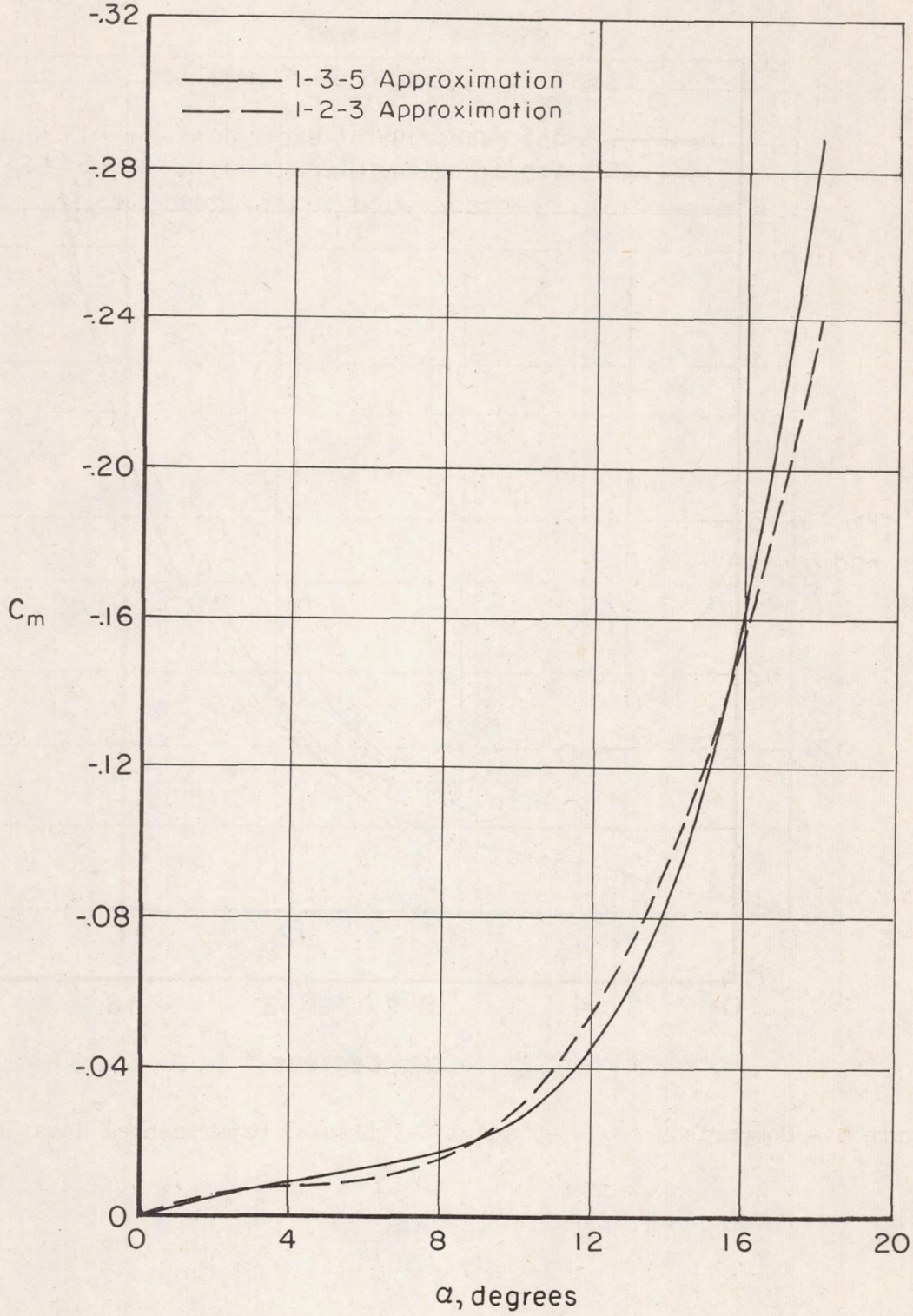

Figure 7.- Restoring moment coefficient corresponding to 1-3-5 and 1-2-3 fits of experimental data.

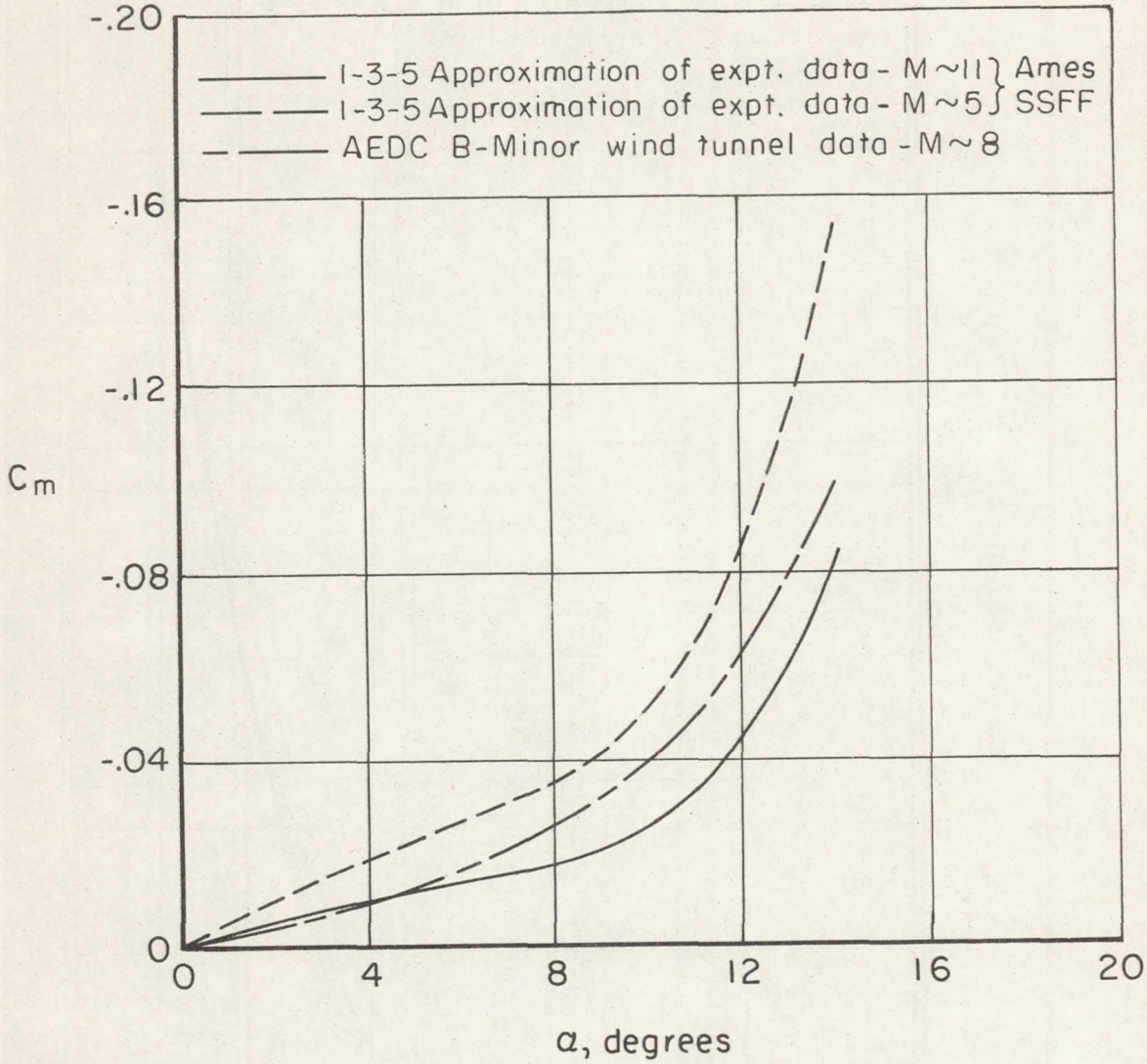

Figure 8.- Comparison of free-flight data with wind-tunnel data.

A
4
7
9

A
4
7
9

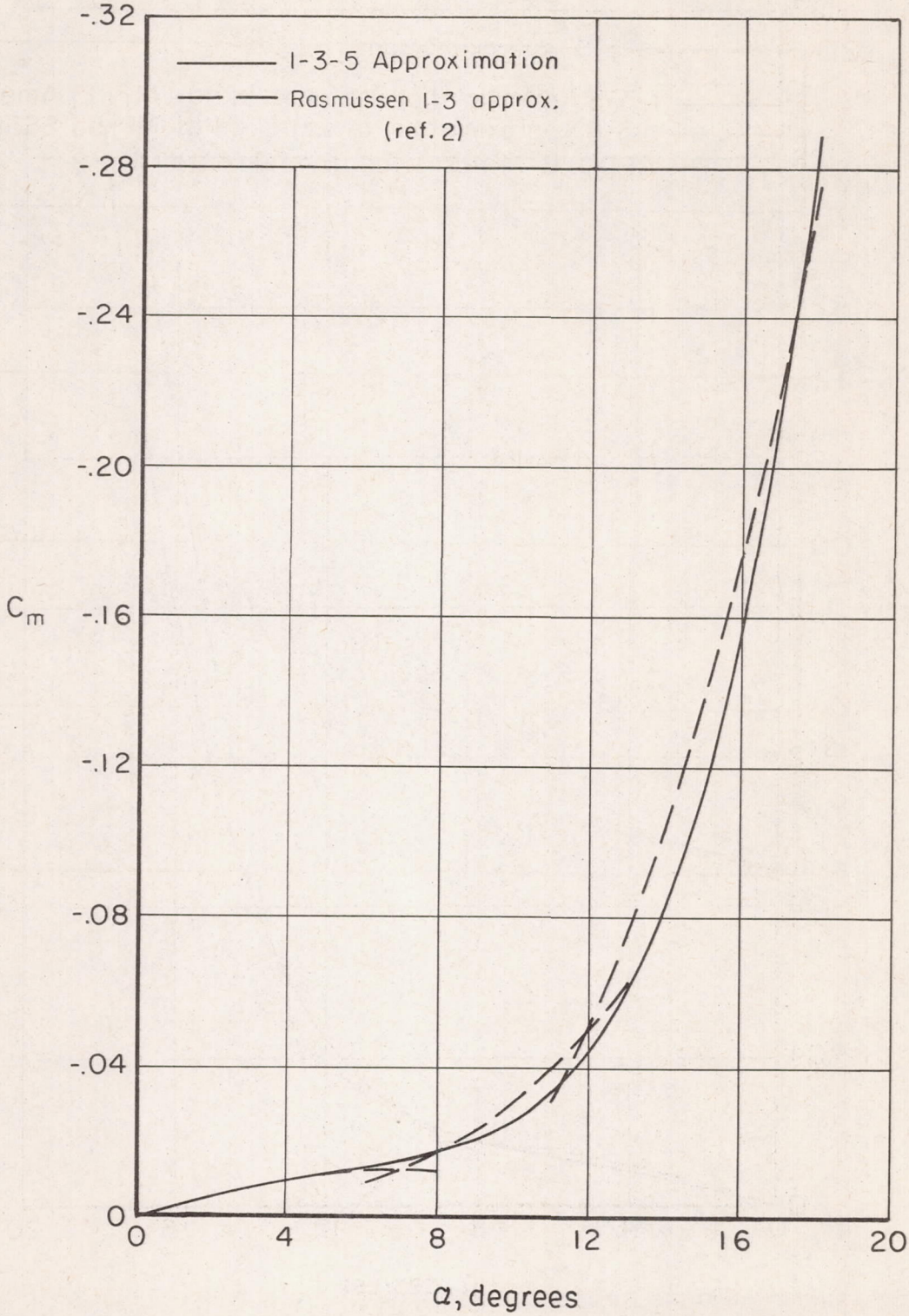

Figure 9.- Comparison of the method of the present report with Rasmussen's method.

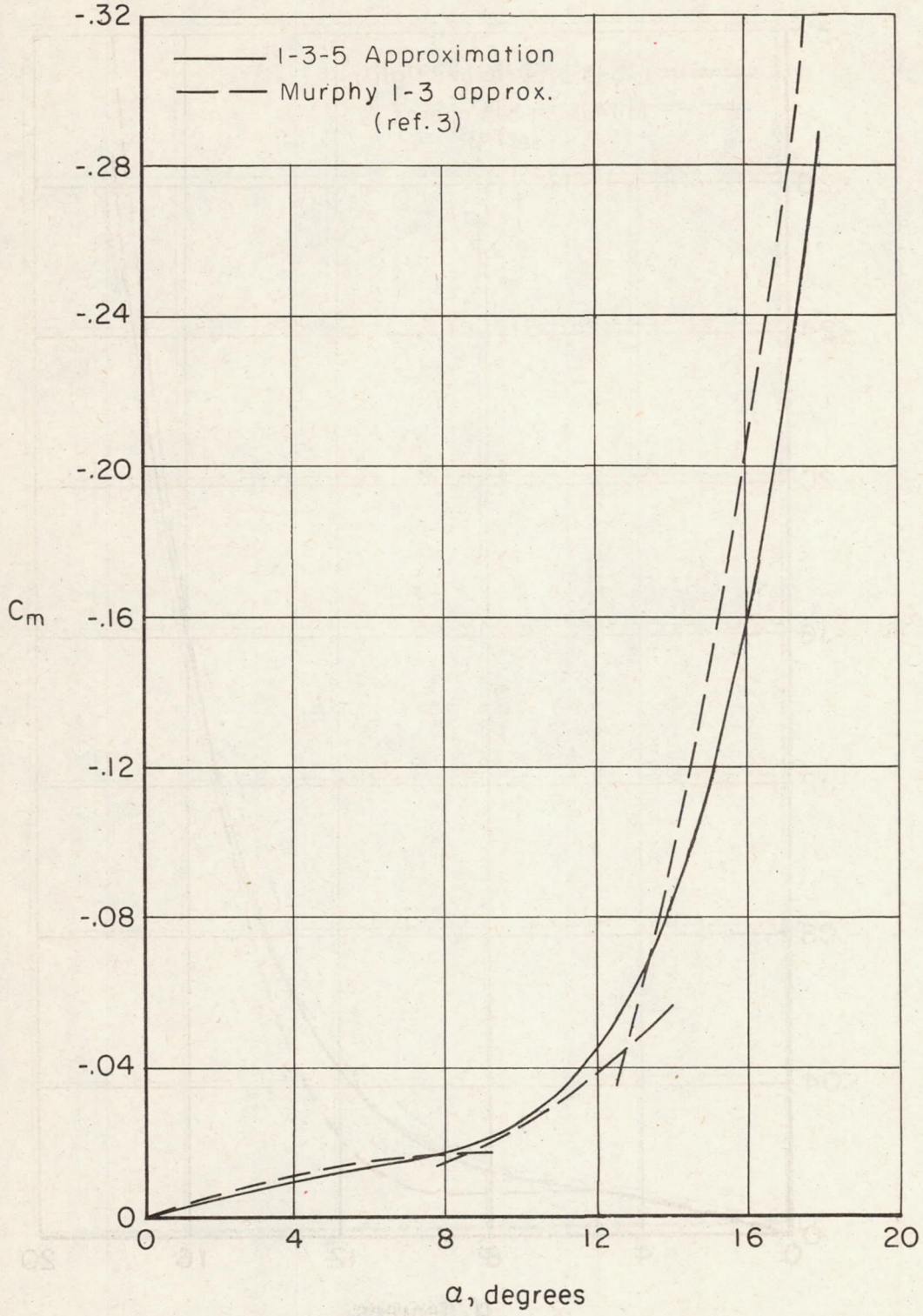

Figure 10.- Comparison of the method of the present report with Murphy's 1-3 method.

A
4
7
9

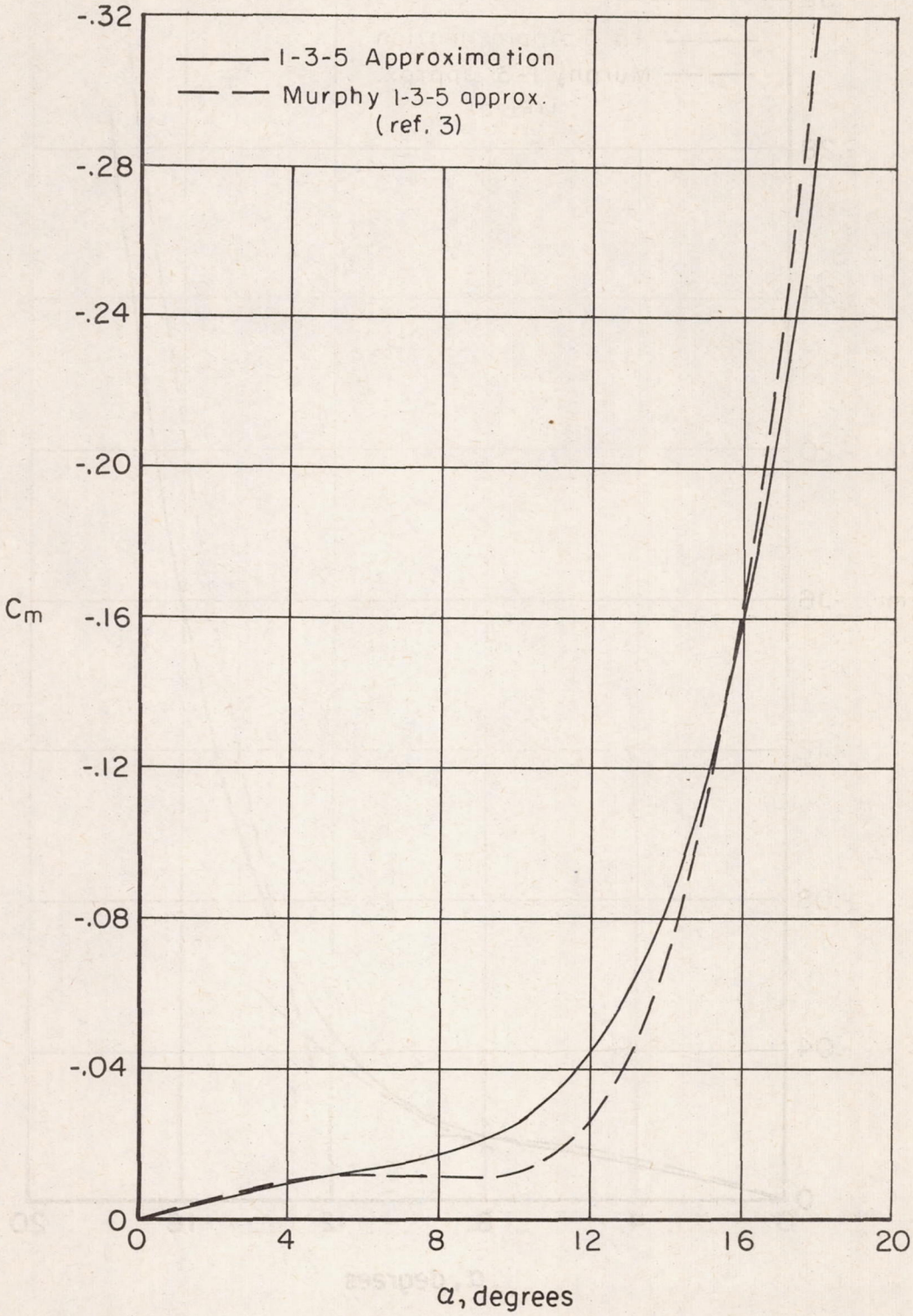

Figure 11.- Comparison of the method of the present report with Murphy's 1-3-5 method.